

Massive binary black holes in galactic nuclei and their path to coalescence

Monica Colpi

25 June 2014, to appear in Space Science Reviews - DOI: 10.1007/s11214-014-0067-1

Abstract Massive binary black holes ($10^5 M_\odot - 10^9 M_\odot$) form at the centre of galaxies that experience a merger episode. They are expected to coalesce into a larger black hole, following the emission of gravitational waves. Coalescing massive binary black holes are among the loudest sources of gravitational waves in the Universe, and the detection of these events is at the frontier of contemporary astrophysics. Understanding the black hole binary formation path and dynamics in galaxy's mergers is therefore mandatory. A key question poses: during a merger, will the black holes descend over time on closer orbits, form a Keplerian binary and coalesce shortly after? Here we review progress on the fate of black holes in both major and minor mergers of galaxies, either gas-free or gas-rich, in smooth and clumpy circum-nuclear discs after a galactic merger, and in circum-binary discs present on the smallest scales inside the relic nucleus.

Keywords black hole physics · dynamics · galaxy mergers · black hole binaries

1 Massive binary black holes as tracers of black hole seed formation and galaxy assembly, along cosmic history

In the universe, *black holes* come in *two flavours*: the "stellar black holes" relic of the most massive stars, weighing $\sim 5 - 30 M_\odot$ (Özel et al. 2010), and the "super-massive black holes" residing in the nuclear regions of galaxies which carry large masses, typically in excess of $10^8 M_\odot$ (Vestergaard et al. 2008). The black holes of stellar origin are observed in X-ray binaries as accreting objects, while the super-massive ones power the bright QSOs and the less luminous active galactic nuclei (AGN) (Merloni and Heinz 2013). Super-massive black holes are also observed in their quiescent state as massive dark objects in nearby galaxy spheroids (Gültekin et al. 2009; Kormendy and Ho 2013), and a compelling case is that of the Milky Way housing an (almost) inactive black hole of $4 \times 10^6 M_\odot$ (Ghez et al. 2008; Gillessen et al. 2009).

Monica Colpi
Department of Physics G. Occhialini
University of Milano Bicocca, Piazza della Scienza 3, I20123, Milano, Italy
Istituto Nazionale di Fisica Nucleare (INFN) - Milano Bicocca, Piazza della Scienza 3, I20123, Milano, Italy
email: monica.colpi@unimib.it

A black hole *desert* exists between $\sim 30 M_{\odot}$ and $\sim 10^6 M_{\odot}$. These black holes are often called *intermediate mass* or *middleweight* black holes with boundaries of the desert zone that are not physically constrained, due to the lack of observations. The *maximum* mass of a black hole of stellar origin can be as large as a few $\times 10^2 M_{\odot}$, according to theoretical studies, depending on the metallicity of the collapsing progenitor stars and on the role of radiative feed-back in limiting the final mass (Omukai and Palla 2001; Heger et al. 2003). The *minimum* mass of super-massive black holes is not constrained as unknown is the process of formation of these black holes (Volonteri 2010; Schleicher et al. 2013).

Limits on the density of the X-ray background light (resulting from accretion of an unresolved population of massive black holes) and on the local black hole mass density (Marconi et al. 2004; Merloni and Heinz 2013), suggest that super-massive black holes have grown their mass across cosmic ages through repeated episodes of accretion and via coalescences driven by galaxy mergers. This has led to the concept of black hole *seed* and black hole growth from seeds in concordance with the rise of cosmic structure. The characteristic mass or mass interval of the seed population is unknown and weakly constrained theoretically. Thus, aim of contemporary astrophysics is to disclose the mechanism of black hole seed formation through the detection of middleweight black holes in galaxies (Reines et al. 2013).

The discovery of tight correlations between the black hole mass M_{\bullet} and stellar velocity dispersion σ_* , and between M_{\bullet} and the stellar mass of the spheroid M_* ($M_{\bullet}/M_* \sim 10^{-3}$) highlighted the existence of a process of symbiotic evolution between black holes and galaxies (Marconi and Hunt 2003; Häring and Rix 2004; Ferrarese and Ford 2005; Gültekin et al. 2009; Kormendy and Ho 2013). The current interpretation is that the huge power emitted by the central black hole when active may have affected the rate of star formation in the host, turning the galaxy into a red and dead elliptical (Mihos and Hernquist 1996; Di Matteo et al. 2005; Hopkins et al. 2006). At present, there is a live debate on whether the correlation extends to bulge-less disc galaxies or in general to lower mass galaxies (Kormendy and Ho 2013). Lower mass galaxies are expected to house lighter super-massive black holes, according to the above relations. Thus low-mass galaxies are the preferred sites for the search of the middleweight black holes in the desert zone. Many galaxies (up to 75%) host at their centre a Nuclear Star Cluster, a compact sub-system of stars with mass M_{NSC} typically $\lesssim 10^7 M_{\odot}$, and half-mass radius of $\lesssim 10$ pc. In a number of Nuclear Star Clusters a central middleweight black hole has been discovered which co-habit the cluster (Ferrarese et al. 2006). Less tight correlations have been found between M_{NSC} and the mass M_* of the host galaxy (Scott and Graham 2013), indicating that while in bright spheroids the presence of a central black hole appears to be compulsory ¹, in less bright (disc) galaxies a Nuclear Star Cluster, with or without a central black hole, is preferred.

The search for middleweight black holes in less massive disc galaxies will be central for understanding the process of formation and co-evolution of black holes and galaxies (Reines et al. 2013; Kormendy and Ho 2013). But, this is not the only strategy. A powerful and promising new route exists to unveil infant black holes, forming at high redshift $z \lesssim 15$: this is the route proposed by *The Gravitational Universe*, the science theme selected by ESA for the next large mission L3, *for the search and detection of*

¹ See Gerosa and Sesana (2014) for missing black holes in the brightest cluster galaxies following black hole coalescence and ejection by gravitational recoil.

low frequency gravitational waves from coalescing binary black holes in merging galactic halos (eLISA Consortium 2013).

According to the current paradigm of the Λ -CDM cosmology, galaxies form following the baryonic infall of gas into collapsing dark matter halos and assemble hierarchically through mergers of (sub-)galactic units (White and Rees 1978). Black hole seeds growing in these pristine merging halos inescapably undergo coalescences (Volonteri et al. 2003). This is illustrated in Figure 1, where we show characteristic tracks of black holes along cosmic history computed from semi-analytical models of galaxy formation (Volonteri and Natarajan 2009). The tracks are reported in the mass versus redshift plane, from $10^2 M_\odot$ up to $10^9 M_\odot$ and for $0 \lesssim z \lesssim 20$: black holes form from seeds of different masses (according to different seed formation models) and grow via accretion and mergers, the last denoted as circles in the diagram. The gravitational wave signal from these mergers will be detected with a high signal-to-noise ratio from the forthcoming science mission of *The Gravitational Universe*, eLISA (eLISA Consortium 2013). This will allow to explore black hole seed formation and evolution as early as $z \gtrsim 10$, just at the end of the dark ages but well before the epoch of cosmic re-ionisation of the intergalactic hydrogen.

Black holes come in binaries when two galaxies merge, and the gravitational wave signal emitted at coalescence offer a unique environment to measure, with exquisite precision, the black hole masses and spins, every time there is a merger (Amaro-Seoane et al. 2013). Thus, it has become mandatory to study how and when binary black holes form and evolve inside galactic halos, during the formation of cosmic structures. This is a multi-face problem crossing the boundaries between astrophysics and cosmology.

This review aims at describing one aspect of the astrophysics of binary black holes: that of their dynamics in merging galaxies. This is a central problem if we want to consider binary black holes as powerful sources of gravitational waves and as unique tracers of the cosmic assembly of galaxies, as proposed in *The Gravitational Universe* (eLISA Consortium 2013). This problem carries some resemblance to the problem of formation, in stellar dynamics, of close binary neutron stars fated to coalesce: rapid shrinking of the star’s orbits occurs through phases of unstable mass transfer and common envelope evolution to avoid the risk of supernova disruption, before the two compact stars reach the phase of inspiral by gravitational waves. Likewise, binary black holes experience a phase of rapid sinking by dynamical friction when the two galaxies merge, but only after experiencing close encounters with stars and strong coupling with gas, they enter the phase of gravitational wave driven inspiral. In the next sections, we will describe the fate of massive black holes in merging galaxies, indicating whether they form close binaries ready to coalesce or wide pairs fated to wander in the host galaxy, and the conditions for this to happen.

Section 2 starts with a brief historical recollection of the problem of black hole dynamics in stellar environments, and expands these early findings to account for recent advances in this field. Section 3 addresses the problem of black hole dynamics in gas-rich galaxy major and minor mergers, while Section 4 describes the fate of black holes in gaseous circum-nuclear and circum-binary gas discs. Section 5 presents a short summary of the timescales along the path to coalescence, and Section 6 contains the main conclusion and the directions in which the field may evolve into.

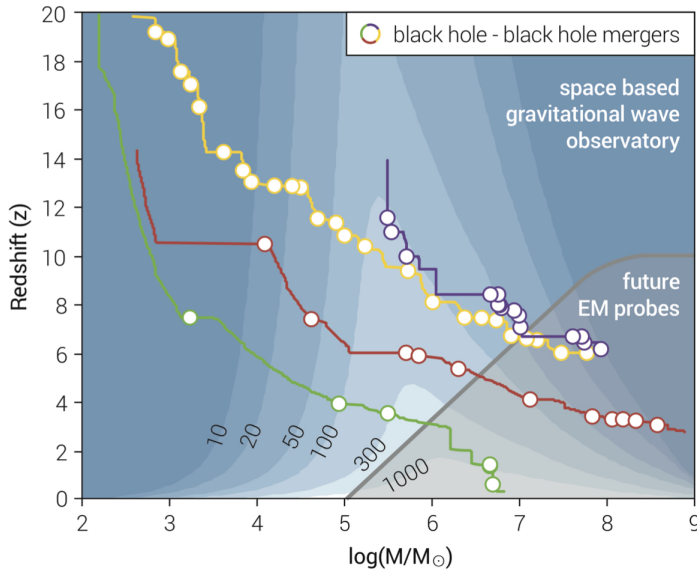


Fig. 1 Paths of black holes forming at high redshift from light ($10^{2-3} M_{\odot}$) and heavy ($10^{5-6} M_{\odot}$) seeds. The black holes evolve along tracks, in the mass versus redshift diagram, as they experience accretion episodes and coalescences with other black holes. Circles mark the loci of black hole coalescences. Four paths are selected: two ending with a black hole powering a $z \sim 6$ QSO (starting from a massive seed, blue curve, and from a seed resulting from the collapse of a massive metal-free star, yellow curve); a third ending with a typical $10^9 M_{\odot}$ black hole in a giant elliptical galaxy (red curve); and finally the forth ending with the formation of a Milky Way-like black hole (green curve). The tracks are obtained using state-of-the-art semi-analytical merger tree models. The grey transparent area in the bottom right corner roughly identifies the parameter space accessible by future electromagnetic probes which will observe black holes powered by accretion. Over-laid are contour levels of constant sky and polarisation angle-averaged Signal-to-Noise-Ratios (SNRs) for eLISA, for equal mass non-spinning binaries as a function of their total rest frame mass (eLISA Consortium 2013). It is remarkable that black hole mergers can be detected by eLISA with a very high SNR across all cosmic ages. Courtesy of eLISA Consortium (2013).

2 Binary black holes in stellar environments

2.1 Super-massive black hole binaries in galactic nuclei

In a pioneering Letter to *Nature*, Begelman, Blandford and Rees (1980) write: "There are straightforward reasons for surmising that super-massive black hole binaries exist: mergers between galaxies appear to be frequent; cD galaxies in clusters or groups quite probably formed in this manner; and there is direct evidence that the near-by active galaxy Centaurus A is a merger product." In particular, they correlate the bending and apparent precession of radio jets, observed in a number of active nuclei, with the presence of two black holes in a binary, exploring the dynamics of its formation inside the violently relaxed *stellar core* of the newly formed galaxy.

Begelman et al. depicted the existence of three main phases along the path to coalescence: an early phase of *pairing* (phase I) under dynamical friction in the stellar bulge of the post-merger galaxy, ending with the formation of a close *Keplerian binary*; a phase of *hardening* (phase II) during which the binary separation decreases due to

energy loss by close encounters with single stars plunging on nearly radial orbits on the binary; a phase of *gravitational wave inspiral* (phase III), ending with the coalescence of the two black holes due to the emission of gravitational waves. In all the phases, gravitational torques act to decrease the orbital angular momentum and energy of the black holes, to promote their pairing and sinking toward more bound states.

The black hole that forms has a new mass, new spin according to mass-energy conservation (Rezzolla et al. 2008) and because gravitational waves carry away linear momentum, the new black hole receives a gravitational recoil that can be as large as $\lesssim 5000 \text{ km s}^{-1}$ depending on the orientation and magnitude of the black hole spins and orbital angular momentum at the time of binary coalescence (Lousto and Zlochower 2013). Thus, an additional phase IV subsequent to merging should be considered corresponding to a *recoiling* black hole moving-inside or escaping-from its host galaxy (Gualandris and Merritt 2008; Merritt et al. 2009; Devecchi et al. 2009). This phase and the relation between spin, mass ratio and recoil are not considered here (Bogdanović et al. 2007; Dotti et al. 2010; Centrella et al. 2010) nor the observability of active black holes along their path to coalescence [we defer the reader to e.g. Komossa (2006); Schnittman (2011); Bode et al. (2010); Eracleous et al. (2011); Liu et al. (2011); Komossa (2012); Koss et al. (2012); Liu et al. (2013); Decarli et al. (2013); Comerford and Greene (2014); Lusso et al. (2014); Liu et al. (2014)].

Returning to phase I, it is known that dynamical friction against the stars acts on each black hole individually to cause their progressive sinking (Chandrasekhar 1943; Begelman et al. 1980; Colpi et al. 1999; Yu 2002), until they come close enough to form a *Keplerian binary*. As dynamical friction is proportional to the background density of stars and to the square of the black hole mass, more massive black holes in denser environments sink more rapidly. In a stellar background of N stars described by a singular isothermal sphere, with density profile $\rho_* = \sigma_*^2 / (2\pi G r^2)$ and one-dimensional (1D) velocity dispersion σ_* , a black hole of mass m_\bullet at distance r sinks by dynamical friction on a timescale

$$\tau_{\text{df}} \sim 2 \times 10^8 \ln^{-1} N \left(\frac{10^6 \text{ M}_\odot}{m_\bullet} \right) \left(\frac{r}{100 \text{ pc}} \right)^2 \left(\frac{\sigma_*}{100 \text{ km s}^{-1}} \right) \text{ yr}. \quad (1)$$

This timescale decreases with decreasing distance from the galaxy's nucleus, so that dynamical friction becomes more and more rapid with orbital decay. Eventually, the black holes end forming a Keplerian system. Binary formation occurs approximately when the mass in stars enclosed in their orbit drops below twice the total mass of the binary $m_{\bullet,t} = m_{\bullet,1} + m_{\bullet,2}$; hereon $m_{\bullet,1}$ ($m_{\bullet,2}$) is the mass of the primary (secondary) black hole, and $q = m_{\bullet,2}/m_{\bullet,1} \leq 1$ the mass ratio. In a singular isothermal sphere, a Keplerian binary forms when $a_{\text{binary}}^* \simeq G m_{\bullet,t} / \sigma_*^2$, i.e. at a separation comparable to the gravitational sphere of influence of the black holes viewed as a single point mass $m_{\bullet,t}$. Dynamical friction guides the inspiral, with no significant amplification of the eccentricity (Colpi et al. 1999), approximately down to a_{binary}^* . The weakening of dynamical friction is due to the high velocity that the black holes acquire when they form a binary, as the drag is inversely proportional to the square of the orbital velocity.

Phase I ends when the binary separation a has decayed below

$$a_{\text{hard}}^* = a_{\text{binary}}^* \frac{\mu}{3m_{\bullet,t}} \sim \frac{G\mu}{3\sigma_*^2} \sim 0.1 \frac{q}{(1+q)^2} \left(\frac{m_{\bullet,t}}{10^6 \text{ M}_\odot} \right) \left(\frac{100 \text{ km s}^{-1}}{\sigma_*} \right)^2 \text{ pc}, \quad (2)$$

where $\mu = m_{\bullet,t}q/(1+q)^2$ is the reduced mass of the binary (Quinlan 1996; Yu 2002; Merritt and Milosavljević 2005). The hardening radius a_{binary}^* is defined as the binary separation at which the kinetic energy per unit mass of the binary equals the kinetic energy per unit mass of the stars in the galactic potential. During the hardening phase II, the black hole orbital energy and angular momentum are extracted via scattering of single stars off the binary, in close three-body encounters. As a single star impinging on the binary causes a fractional energy change of the order of $\sim \xi m_*/m_{\bullet,t}$ (where $\xi \sim 0.2 - 1$ is a coefficient calculated after averaging over many star-binary scattering experiments), a large number of stars, or the order of $\sim m_{\bullet,t}/m_*$, is necessary for a sizeable change of the binary binding energy $E_{\bullet} = Gm_{\bullet,1}m_{\bullet,2}/2a$. The binary offers a cross section $A \sim \pi a Gm_{\bullet,t}/\sigma_*^2$ to the incoming flow of stars and this leads to a hardening rate $s \equiv d(1/a)/dt \sim \xi \pi G \rho_*/\sigma_*$ for the semi-major axis a , and a corresponding hardening time (independent on the number N of stars in the galaxy)

$$\tau_{\text{hard}}^* \sim \frac{\sigma_*}{\pi G \rho_* a} \sim 70 \left(\frac{\sigma_*}{100 \text{ km s}^{-1}} \right) \left(\frac{10^4 \text{ M}_{\odot} \text{ pc}^{-3}}{\rho_*} \right) \left(\frac{10^{-3} \text{ pc}}{a} \right) \text{ Myr}. \quad (3)$$

Opposite to τ_{df} , the hardening time τ_{hard}^* increases with decreasing a , as the binary cross section decreases with a . Thus, a potential stalling of the binary can occur at the smallest binary separations, during phase II.

Phase III starts when the coalescence time driven by gravitational wave emission

$$\tau_{\text{gw}} \sim 5.4 \times 10^8 f(e)^{-1} \frac{(1+q)^2}{q} \frac{a^4}{m_{\bullet,t}^3} \left(\frac{1}{0.001 \text{ pc}} \right)^4 \left(\frac{10^6 \text{ M}_{\odot}}{m_{\bullet,t}} \right)^3 \text{ yr} \quad (4)$$

drops below τ_{hard}^* , where $f(e) = [1 + (73/24)e^2 + (37/96)e^4](1 - e^2)^{-7/2}$. The crossing condition, $\tau_{\text{hard}}^* = \tau_{\text{gw}}$ thus provides the binary separation at which the black holes transits from phase II into III:

$$a_{\text{II} \rightarrow \text{III}}^* = \left(\frac{G^2}{c^5} \frac{256}{5\pi} \right)^{1/5} \left(\frac{\sigma_*}{\rho_*} \right)^{1/5} f^{1/5}(e) \left(\frac{q}{(1+q)^2} \right)^{1/5} m_{\bullet,t}^{3/5}. \quad (5)$$

If τ_{gw} evaluated at $a_{\text{II} \rightarrow \text{III}}^*$ exceeds the age of the universe, than the binary *stalls* and does not reach coalescence. From equation [4], we can define as a_{gw} the distance at which the coalescence time τ_{gw} equals the Hubble time τ_{Hubble} :

$$a_{\text{gw}} = 2 \times 10^{-3} f(e)^{1/4} \frac{q^{1/4}}{(1+q)^{1/2}} \left(\frac{m_{\bullet,t}}{10^6 \text{ M}_{\odot}} \right)^{3/4} \left(\frac{\tau_{\text{Hubble}}}{13.6 \text{ Gyr}} \right)^{1/4} \text{ pc}. \quad (6)$$

Expressed in units of the Schwarzschild radius $r_S = 2Gm_{\bullet,t}/c^2$ associated to $m_{\bullet,t}$, $a_{\text{gw}} = 1.4 \times 10^4 (m_{\bullet,t}/10^6 \text{ M}_{\odot})^{-1/4} r_S$ for the case of an equal mass circular binary. Coalescence occurs as long as $a_{\text{II} \rightarrow \text{III}}^* < a_{\text{gw}}$.

According to equation [3], for a wide interval of stellar densities and velocity dispersions, the coalescence time τ_{gw} , evaluated at $a_{\text{II} \rightarrow \text{III}}^*$, is less than the Hubble time τ_{Hubble} , so that the binary is expected to enter the gravitational wave driven regime shortly after it has become hard. However, the estimate of τ_{hard}^* , in equation [3], severely *underestimates the true hardening time* since a large number of stars in "loss cone" orbits is necessary to drive the binary down to phase III. The loss cone in the black hole binary system is identified as the domain, in phase-space, populated by stars with sufficiently low angular momentum, $J^2 \lesssim J_{\text{lc}}^2 \lesssim 2Gm_{\bullet,t}a$, to interact with the binary. If

hardening occurs at a constant rate s , the number of stars necessary to complete the hardening phase is as large as $N^{1c} \sim (\mu/m_*) \ln(a_{\text{hard}}^*/a_{\text{gw}})$, comparable to the mass of the binary. In the case of massive black holes ($m_{\bullet,t} > 10^8 M_\odot$) in elliptical galaxies and spheroids, such a large reservoir of stars may *not* be available (Merritt 2013b).

At the end of phase I, when stellar encounters begin to control the contraction of the newly formed binary, the black holes start ejecting stars from the loss cone at a high clearing rate. Refilling of stars in the phase-space requires a lapse time comparable to the two-body relaxation timescale $\tau_{\text{rel}} \propto N$ which in galactic nuclei, viewed as spherical systems, is often longer than the Hubble time (Yu 2002). Thus, the lack of stars in phase-space causes the binary to *stall*, at a separation a_{stall}^* typically of $\sim 0.1 - 1$ pc, much larger than a_{gw} (eq. [6]). Thus the binary can not reach coalescence in a Hubble time, and this is referred to as *the last parsec problem*. This represents an obstacle to the path to coalescence during the transit across phases II and III, for a large range of black hole masses, and mass ratios q (Yu 2002). We are therefore left with a major uncertainty on the estimate of the *true hardening time* τ_{Hard} which is expected to be closer to τ_{rel} , in the case of empty loss cone, and to τ_{hard}^* as given by equation [3], in the case of full loss cone: thus, $\tau_{\text{hard}}^* < \tau_{\text{Hard}} < \tau_{\text{rel}}$.

The binary is a source of kinetic energy as it deposits in the stellar bath an energy

$$\Delta E_\bullet \sim E_\bullet(a_{\text{gw}}) \sim 2 \times 10^{55} f(e)^{-1/4} \frac{q^{3/4}}{(1+q)^{3/2}} \left(\frac{m_{\bullet,t}}{10^6 M_\odot} \right)^{5/4} \left(\frac{\tau_{\text{Hubble}}}{13.6 \text{ Gyr}} \right)^{-1/4} \text{ erg}, \quad (7)$$

in order to enter phase III. Compared to the binding energy of a stellar bulge of mass M_* , $(3/2)M_*\sigma_*^2$, energy deposition accounts $\sim 10\%$ of the total energy of the system, if one assumes $m_{\bullet,t} \sim 10^{-3}M_*$, a value of $\sigma_* \sim 100 \text{ km s}^{-1}$, and an equal mass binary of $10^6 M_\odot$. Binary energy deposition via encounters with single stars can create a stellar core in an otherwise steep density profile, due to star's ejection. Stellar scouring has been observed in a number of core, missing-light elliptical galaxies that are at present indirect candidates for black hole mergers (Milosavljević and Merritt 2001; Kormendy and Ho 2013; Merritt 2013a). The binary carries a larger angular momentum at a_{hard}^* compared to the angular momentum at the onset of gravitational wave inspiral,

$$\frac{J_\bullet(a_{\text{hard}}^*)}{J_\bullet(a_{\text{gw}})} \sim 10 (1-e^2)^{7/16} \frac{q^{3/8}}{(1+q)^{3/4}} \left(\frac{m_{\bullet,t}}{10^6 M_\odot} \right)^{1/8} \frac{100 \text{ km s}^{-1}}{\sigma_*} \left(\frac{\tau_{\text{Hubble}}}{13.6 \text{ Gyr}} \right)^{-1/8}. \quad (8)$$

From the equation it is clear that the binary can reduce J_\bullet when transiting from phase II to III, increasing the eccentricity during orbital decay.

After Begelman et al., the last parsec problem has been considered a major bottleneck to the path of binary coalescence, and has motivated many studies (Milosavljević and Merritt 2001; Yu 2002; Merritt and Milosavljević 2005). Direct N -Body simulations of binary inspiral in isotropic, spherical galaxy models confirmed, on solid grounds, the stalling of the binary: the binary hardening rate s was found to be proportional to the rate of repopulation of loss cone orbits which in turn depends on N . Simulations with a lower number of particles N (corresponding to shorter two-body relaxation times τ_{rel}) show rapid binary decay. By contrast, more realistic simulations with larger N (longer τ_{rel}) display a much lower hardening rate s for the binary (Preto et al. 2011). The extrapolation of the result to the limit of very large N , as in elliptical galaxies or bulges of spirals, leads to stalling of the massive binary over a Hubble time.

Yu (2002) noticed that if one drops the assumption of sphericity, the hardening time τ_{Hard} is lower and can be less than the Hubble time in the case of less massive (power-law) galaxies which have a shorter τ_{rel} . Spherical galaxies have all stars on centrophobic orbits, whereas galaxies with a high degree of axisymmetry and triaxiality host a significant fraction of stars on centrophilic orbits, such box orbits, which pass arbitrarily close to the binary and have low angular momentum. Furthermore, chaotic orbits in steep triaxial potentials can enhance the mass flux into the loss cone region (Merritt and Poon 2004). Some non axisymmetric potential can also excite bar instabilities causing a flow of stars toward the binary (Berczik et al. 2006).

Binary stalling has been recently challenged in models of galaxy’s mergers. A number of direct N -Body simulations indicate that the end-product of a merger is not a spherical galaxy (Berczik et al. 2006; Khan et al. 2011; Preto et al. 2011; Khan et al. 2013; Wang et al. 2014). The new galaxy retains substantial amount of rotation or/and a large degree of asphericity or triaxiality such that the binary is seen to harden at a rate independent of N , as if the loss cone were fully refilled, or as if an N -independent mechanism (collisionless relaxation) provides a supply of stars in loss cone orbits. In light of these findings the last parsec problem appears today as an artefact of the oversimplifying assumption of sphericity of the relic galaxy, and that more realistic models, simulated starting from *ab initio* conditions, point in the direction of hardening times ranging between 0.1 and a few Gyrs, for the models explored.² An interesting corollary of these investigations is that in non-spherical models the binary eccentricity e is seen to increase to values very close to 1 (Preto et al. 2011; Khan et al. 2011), indicating rapid transfer of angular momentum to stars from the cumulative action of many scatterings (Sesana 2010; Dotti et al. 2012).

As final remark, alternative mechanisms exist that can cause the contraction of the binary orbit, such as recycling of stars ejected by the binary on returning eccentric orbits (Milosavljević and Merritt 2003), massive perturbers scattering stars into loss cone orbits (Perets et al. 2007), or a third black hole in a trio encounter. In the latter case, the third closely interacting black hole can harden the binary due to eccentricity oscillations (Blaes et al. 2002), or energy exchange in the three-body scattering, or can repopulate the loss cone having perturbed the underlying gravitational potential of the host galaxy (Hoffman and Loeb 2007; Kulkarni and Loeb 2012).

So far, we considered the hardening of massive black hole binaries in massive galaxies. But, a question to investigate is related to the evolution of middleweight black holes of $\sim 10^{3-4} M_{\odot}$ which tend to inhabit smaller mass halos with shorter relaxation timescales, and that form at high redshift when the universe was younger. This narrows down the interval of time accessible for hardening. Is there a last parsec problem? Extrapolating the results to middleweight black hole masses may not be straightforward, and in the next subsection we shortly explore the hardening in this regime.

² This view, however, has been criticised by Vasiliev et al. (2013) who compared the evolution of binary black holes in spherical, axisymmetric and triaxial equilibrium galaxy models. They find that the rate of binary hardening exhibits a significant N -dependence in all the models, in the investigated range of $10^5 \leq N \leq 10^6$. Their hardening rates are substantially lower than those expected if the binary loss cone remained full, with rates between the spherical and non-spherical models differing in less than a factor of two. This finding seems to cast doubt on claims that triaxiality or axisymmetry alone are capable of solving the final-parsec problem. Vasiliev and co-authors invite caution in extrapolating results to galaxies with high values of N until all discrepancies or intrinsic differences between equilibrium models and merged galaxy models are not understood deeply.

2.2 Middleweight binary black holes in stellar environments: hardening or stalling in high redshift nuclei?

Studying the hardening and coalescence of middleweight black hole binaries with $m_{\bullet,t} \gtrsim 10^4 M_\odot$ is of importance as black holes of this mass are primary sources for eLISA, as illustrated in Figure 1. In the figure, black hole coalescences occur at a rate equal to the rate of merging of their parent dark matter halos controlled by dynamical friction only. The underlying assumption is there is no or negligible delay between the merger of the halo and that of the nested black holes, caused by the potential stalling of the binary. At present, whether black hole binaries at very high redshift are able to reach coalescence in the short cosmological time lapse between black hole seed formation and halo mergers is unclear (paper in preparation).

As an exercise and for illustrative purposes, one can compute limits upon the density ρ_* and velocity dispersion σ_* that a massive stellar cluster should have to allow rapid hardening of the binary during phase II. In star clusters the density and velocity dispersion are functions of distance. Thus, one should consider ρ_* and σ_* are characteristic values of the central region of a massive star cluster in an hypothetical galactic nucleus.

Focus on the case of a black hole forming at z_{form} (e.g. ~ 20) and coalescing with another black hole, following a halo-halo merger at z_{coal} (~ 15), or the case of two adjacent mergers between redshift z_1 and z_2 over a short interval of cosmic time. The time lapse $\Delta\tau_{\text{lapse}}$ can be as short as $\lesssim 0.1$ Gyr, or more conservatively as short as 1 Gyr. In Figure 2 we plot, in the $\sigma_* - \rho_*$ plane, the lines of constant $\tau_{\text{rel}} = 0.34\sigma_*^3/(G^2 m_* \rho_* \ln \Lambda)$ (with $m_* = 1 M_\odot$ and $\ln \Lambda \sim 10$) corresponding to a cosmic time lapse $\Delta\tau_{\text{lapse}}$ equal to 0.1 Gyr and 1 Gyr, respectively. The solid lines in Figure 2 refer to the loci where $\tau_{\text{rel}} = \Delta\tau_{\text{lapse}}$, so that characteristic densities higher than

$$\left(\frac{\rho_*}{1.6 \times 10^7 M_\odot \text{pc}^{-3}}\right)_{\text{rel}} \gtrsim \left(\frac{\sigma_*}{100 \text{ km s}^{-1}}\right)^3 \left(\frac{0.1 \text{ Gyr}}{\Delta\tau_{\text{lapse}}}\right) \quad (9)$$

are requested, at a fixed σ_* , to allow for binary hardening on the relaxation timescale (corresponding to the empty loss cone regime). The dashed lines in Figure 2 refer instead to the loci where $\tau_{\text{hard}}^*(a_{\text{gw}}) = \Delta\tau_{\text{lapse}}$, as given by equation [3] (corresponding to the full loss cone regime), for a black hole binary of $m_{\bullet,t} = 10^4 M_\odot$ (upper dashed curve for $\Delta\tau_{\text{lapse}}$ equal to 0.1 Gyr, lower dashed curve for 1 Gyr). This condition implies

$$\left(\frac{\rho_*}{6 \times 10^6 M_\odot \text{pc}^{-3}}\right)_{\text{hard}} \gtrsim \left(\frac{\sigma_*}{100 \text{ km s}^{-1}}\right) \left(\frac{10^4 M_\odot}{m_{\bullet,t}}\right)^{3/4} \left(\frac{0.1 \text{ Gyr}}{\Delta\tau_{\text{lapse}}}\right)^{5/4}. \quad (10)$$

Figure 2 shows that true hardening, at early cosmic epochs, requires densities in excess of $\gtrsim 10^{6-8} M_\odot \text{pc}^{-3}$ and comparatively low dispersion velocities $\lesssim 70 \text{ km s}^{-1}$ to meet the conditions for coalescence in the short time lapse $\Delta\tau_{\text{lapse}}$ of 0.1 or 1 Gyr. We do not know if such dense stellar environment were present at the centre of unstable pre-galactic discs. Today Nuclear Star Clusters, plausible candidates to harbour a central middleweight black hole, have all densities and velocity dispersions that do not meet this condition. Non-equilibrium conditions and/or the presence of gas, abundant in pre-galactic discs, may be instrumental in taxing the black holes to small separations, in this interval of masses, and at earlier cosmic epochs. Thus, a key question to pose is whether *gas* can *fasten* the transition along the three phases of pairing, hardening and

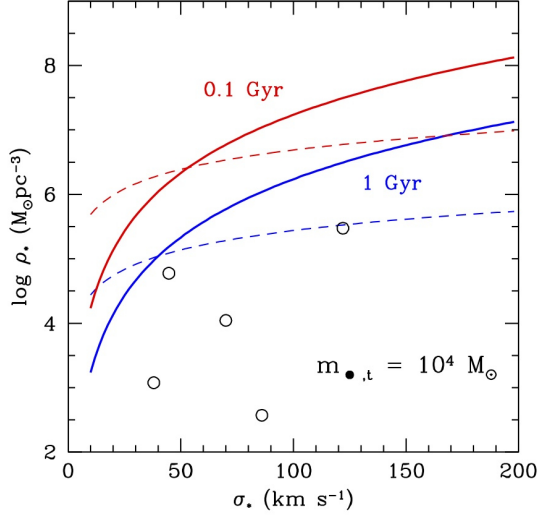


Fig. 2 Stellar mass density (in units of $M_{\odot} \text{ pc}^{-3}$) versus velocity dispersion (in units of km s^{-1}) of hypothetical nuclear star clusters hosting middleweight black hole binaries on their path to coalescence which harden via single-binary encounters with solar mass stars: solid lines refer to the loci in the (σ_*, ρ_*) plane given by eq. 9 where the central relaxation time τ_{rel} equals $\Delta\tau_{\text{lapse}}$. The upper-red (lower blue) solid line refers to $\tau_{\text{rel}} = \Delta\tau_{\text{lapse}} = 0.1$ Gyr (1 Gyr). Dashed lines refer to an equal-mass black hole binary of $10^4 M_{\odot}$ and refer to the loci where the hardening time τ_{hard}^* , given by eq. [3], equals $\Delta\tau_{\text{lapse}}$. The hardening time is computed at a black hole binary separation a_{gw} given by eq. [6]. The upper (lower) dashed line refers to $\tau_{\text{hard}}^* = \Delta\tau_{\text{lapse}} = 0.1$ Gyr (1 Gyr). Empty circles refer to mean stellar densities and velocity dispersion (calculated using the virial theorem) for five Nuclear Star Clusters of known mass and half-mass radii (Seth et al. 2008; Merritt 2013b).

gravitational wave driven inspiral and this question will be addressed in the incoming sections.

3 Black holes dynamics in gas-rich mergers

Merging galaxies which are the sites of formation of binary black holes are expected to contain large concentrations of cold gas (unless one considers mergers between today elliptical galaxies only). This inevitable abundance of gas, in particular in high redshift disc galaxies, motivated us to inquiry into the role of gas dynamics as an alternative in the process of black hole hardening and coalescence.

In this section, we review the pairing of black holes in gas-rich merging galaxies following their dynamics *ab initio* to highlight the key role played by gas in affecting the black hole inspiral and the remarkable difference between *major* and *minor* mergers.

Major mergers refer to interactions between galaxies of comparable mass, while minor mergers refer to interactions between a primary massive galaxy and a less massive galaxy, typically with mass ratio 1:10, and below. Boundaries among major or minor mergers are not sharp, as in many cases, the various outcomes depend also on the internal structure and gas content of the interacting galaxies.

3.1 Major mergers and the formation of a Keplerian binary

The study of black hole dynamics in *gas-rich mergers* dates back to (Mayer et al. 2007), yet it is still in its infancy. The rich physics involved and the high computational demand require state-of-the-art simulations, and the body of data is still inhomogeneous, fragmented and incomplete. While black hole dynamics in collisionless mergers of spherical galaxies has been explored (with direct N -Body codes) starting from galaxies on close elliptical bound orbits and followed mainly during the hardening phase (Khan et al. 2011), black hole dynamics in mergers between gas-rich disc galaxies has been studied starting from cosmologically motivated (parabolic) orbits, during the pairing phase over separations $\gtrsim 10$ kpc, down to the scale ($\lesssim 10$ pc) when the black holes form a Keplerian binary (Mayer et al. 2007; Colpi et al. 2009; Colpi and Dotti 2011; Chapon et al. 2013; Mayer 2013). Further hardening has been later explored in dedicated simulations (Escala et al. 2005; Dotti et al. 2006, 2007, 2009; Fiacconi et al. 2013).

Disc galaxies, as observed at low redshifts, are multi-component systems comprising a collisionless dark matter halo, a stellar disc which coexists with a multi-phase gaseous disc, and a central bulge housing (when present) a massive black hole. Simulating a collision between two disc galaxies with central black holes thus requires simulating the dynamics of the collisionless components (dark matter and stars) jointly with that of gas which is dissipative, and thus subject to cooling, star formation, shock heating and stellar feed-back.

There are many simulations of disc galaxy mergers in the literature (e.g. (Hopkins et al. 2013)), but there exists only a limited number in which the black hole dynamics is followed self-consistently from the \gtrsim kpc scale down to scales $\lesssim 10$ pc. When two galaxies merge, the two black holes are customarily assumed to merge promptly and form a single black hole. A recent set of N -Body/Smooth Particle Hydrodynamic simulations exists which follow the dynamics of black holes from the 100 kpc scale, typical of a merger, down to a scale $\lesssim 10$ pc, and which include star formation and feed-back (Van Wassenhove et al. 2012, 2014). There exists a further class of SPH or/and Adaptive Mesh Refinement (AMR) simulations which have enough resolution to witness the formation of a Keplerian binary on the ~ 1 pc scale, but which treat the gas thermodynamics via a phenomenological energy equation, in the form of a polytrope (Mayer et al. 2007; Chapon et al. 2013).

Equal mass mergers are disruptive for both progenitor galaxies. The galaxies first experience a few close fly-by during which tidal forces start to tear the galactic discs apart, generating tidal tails and plumes. The discs sink by dynamical friction against the dark matter background, and the massive black holes follow passively the dynamics of the bulge and disc they inhabit. Prior to merging, during the second pericentre passage, strong spiral patterns appear in both the stellar and gaseous discs: non axisymmetric torques redistribute angular momentum so that as much as 60% of the gas originally present in each disc of the parent galaxy is funnelled inside the inner few

hundred parsecs of the individual galaxy centres. The black holes, still in the pairing phase, are found to be surrounded by a rotating stellar and gaseous disc.

Later, the gaseous discs eventually merge in a *single massive rotationally supported nuclear disc* of $\lesssim 100$ pc in size, now weighing $\sim 10^9 M_\odot$. The disc develops gravoturbulence (with velocities $\sim 60 - 100 \text{ km s}^{-1}$) that guarantees a Toomre parameter $Q \gtrsim 2$. This prevents fragmentation of gas into stars on the timescale necessary for the black holes to form a Keplerian binary (a few Myr). This short sinking timescale comes from the combination of two facts: that gas densities are higher than stellar densities due to the dissipative nature of the interaction, and that the black holes move relative to the background with mild supersonic velocities. Under these conditions, the hydrodynamical drag is the highest (Ostriker 1999). The subsequent evolution is described in Section 4.

During final revision of this review, a new dedicated N -Body/SPH simulation by (Roškar et al. 2014) of two Milky-Way-like galaxy discs with moderate gas fractions, has been carried out at parsec-scale resolution, including a new model for radiative cooling and heating in a multi-phase medium, star formation and feedback from supernovae. The massive black holes weighing $\sim 10^6 M_\odot$ are form a pair at a separation of ~ 100 pc which gradually spirals inward. However, due to the strong starburst triggered by the merger, the gas in the centre most region is evacuated, requiring ~ 10 Myr for the nuclear disc to rebuild. The clumpy nature of the interstellar medium has a major impact on the dynamical evolution of the pair now subjected to stochastic torquing by both clouds and spiral modes in the disc. These effects combine to delay the orbital decay of the two black holes, just in phase I of gas-dominated dynamical friction. An inspiral timescale of ~ 100 Myr is found in this simulation which is smaller compared to that estimated in collisionless mergers, but longer of a factor at least 10 compared to the case of mergers with a single-phase gas. The result is in line with what found in Fiacconi et al. (2013) (see Section 4.1.2) who describes black hole dynamics in clumpy nuclear discs. We notice however that a single run may not suffice to pin down the characteristic gas-dynamical friction timescale in dissipative mergers, and that the perturbations induced by a population of massive clumps in the stellar component may alter the star's dynamics, prompting rapid refilling of the loss cone region around the two black holes, an effect that these simulations can not capture.

3.2 Black hole paring in unequal-mass mergers

3.2.1 Collisionless unequal-mass mergers

Early works on collisionless mergers of unequal-mass spherical dark matter halos (Governato et al. 1994; Taffoni et al. 2003; Boylan-Kolchin et al. 2008) indicated that additional mechanisms are present, besides dynamical friction, that influence the structure and orbital evolution of the interacting halos (primarily the less massive, secondary): (i) progressive mass loss, or *tidal stripping*, induced by the tidal field of the main halo which reduces the mass of the secondary delaying the sinking by dynamical friction (the force scaling as the square of the satellite mass), and (ii) *tidal heating*, i.e. the effect of short impulses imparted to bound particles within the secondary satellite galaxy by the rapidly varying tidal force of the primary which heats the system causing its (partial) dissolution (Taffoni et al. 2003). Depending on the energy E of the orbit and its degree of circularity ε , on the relative mass concentration c_s/c_h between satellite and main

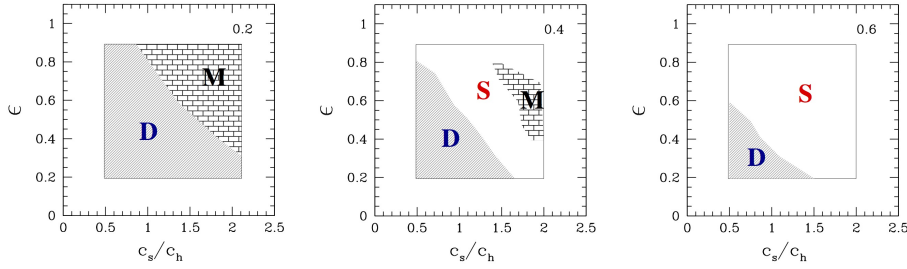


Fig. 3 Outcome of simulations of unequal mass mergers between spherical (dark matter) halos described with a NFW profile (Navarro et al. 1996), and described in the plane circularity ε versus relative concentration c_s/c_h (measuring the ratio between the scale radii of the two halos, defined as in (Navarro et al. 1996; Taffoni et al. 2003)). The figure depicts the life diagram of a satellite halo with mass $M_s/M_h = 0.01$. Each plot is labelled by the value $x(E)$, the radius of the circular orbit (in units of the half mass of the main halo) at the onset of dynamical evolution. We identify the regions corresponding to merger (M) of the satellite into the main host halo, disruption against the background (D), and survival (S) of part of the satellite in the periphery of the main halo. Satellite halos with low concentration on less circular orbits are fragile to disruption, while satellite halos on wide orbits and high concentration preserve their identity. Mergers are preferred in correspondence of high concentration and close circular orbits. Courtesy of Taffoni et al. (2003).

halo, and on the initial mass ratio of the primary to the satellite halos M_h/M_s , the encounter can lead either to rapid merging toward the centre of the primary halo (M), disruption (D), or survival (S) (when a residual mass remains bound and maintains its identity, orbiting in the main halo for a time longer than the Hubble time). Figure 3 illustrates the various outcomes of these experiments. In this context, merging times can be described by an empirical equation which accounts for the progressive mass loss of the secondary by tidal stripping and the progressive delay in the halo merging process

$$\frac{\tau_{\text{df,tidal}}}{t_{\text{dyn}}} \approx \frac{\Theta(E, \varepsilon, c_s/c_h)}{\ln(1 + M_h/M_s(t))} \frac{M_h}{M_s(t)} \quad (11)$$

where Θ , function of the initial parameters, and satellite mass $M_s(t)$ are computed from the numerical simulation. Figure 3 shows the fragility of less concentrated satellites to dispersal and disruption. These findings anticipate the possibility that unequal-mass mergers may release black holes on peripheral orbit inside the primary, due to tidal stripping of the less massive galaxy prior completion of the merger.

3.2.2 Gas-rich unequal-mass mergers

Recent suites of N -Body/SPH simulations of unequal-mass galaxy mergers have highlighted the occurrence of new key features in the dynamics of the discs and their embedded black holes that can be ascribed to differences in the central concentration of the interacting galaxies, and to the geometry of the encounter, but that go beyond the results inferred in Section 3.2.1. These new simulations illustrate the pivotal role played by gas which acts, through its cooling, to enhance the central mass concentration of the satellite and favours the sinking of the secondary black hole in the otherwise disrupted galaxy (Kazantzidis et al. 2005; Callegari et al. 2009, 2011; Van Wassenhove et al. 2012, 2014).

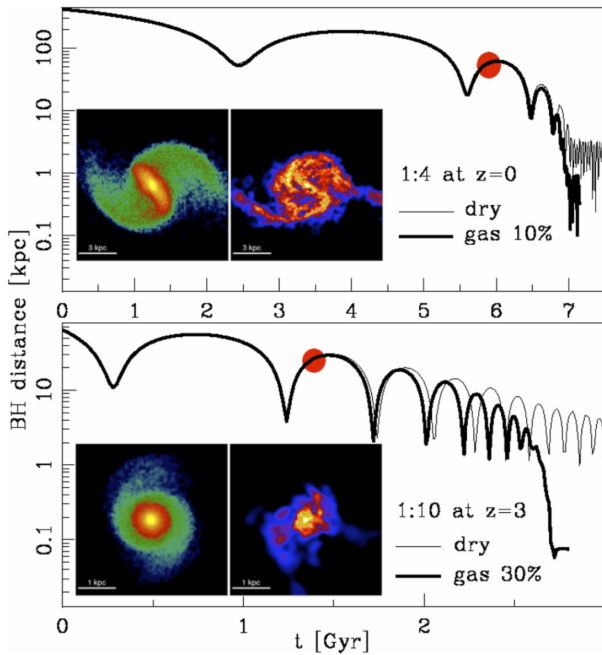


Fig. 4 Upper panel: black hole separation as a function of time for a 1:4 merger. The thin and thick lines refer to the dry (gas free) and wet (with gas fraction of 10%) cases, respectively. The inset shows the color-coded density of stars (left) and gas (right) for the wet case at $t = 5.75$ Gyr (marked with a red dot on the curve); each image is 12 kpc on a side, and colors code the range $10^{-2} - 1 M_{\odot} \text{ pc}^{-3}$ for stars, and $10^{-3} - 10^{-1} M_{\odot} \text{ pc}^{-3}$ for the gas. Lower panel: black hole separation as a function of time for a 1:10 merger (upper panel). The thin and thick line refer to the dry and wet (with gas fraction of 30%) cases, respectively. The inset shows density maps at $t = 1.35$ Gyr for the wet merger: images are 4 kpc on a side (color coding as in upper panel). Courtesy of Callegari et al. (2009).

In unequal-mass mergers, the secondary, less massive galaxy undergoes major transformations. In particular, if the merger is wet, i.e. if the gas fraction in the disc of the secondary is relatively high ($\gtrsim 10\%$), tidal torques during the last peri-centre passage prior merging, trigger inflows which give rise to a nuclear starburst in the vicinity of the secondary black hole. This enhances the resilience of the galaxy’s nucleus against tidal stripping due to the increased stellar density and degree of compactness of the nuclear bulge, at the time the secondary starts interacting with the disc of the primary. The denser stellar cusp surrounding the secondary black hole thus sinks rapidly toward the primary, dragging the black hole that reaches a separation of ~ 100 pc, close to the resolution limit of the simulation. This is illustrated in Figure 4 for 1:4 and 1:10 wet mergers, where the relative separation of the black holes is plotted against time (heavy solid line). In Figure 4 we also plot the stellar and gas distribution at the end of the nuclear starburst that created a denser stellar nucleus in the secondary. The disc of the secondary, rather turbulent and clumpy due to star formation, is later disrupted by ram pressure stripping by the gas of the primary. The secondary black hole continues its sinking toward the centre of the primary, being surrounded by the compact and massive star cluster. In Figure 4, we also contrast the results from dry, i.e. gas free mergers. In the absence of the central starburst, dry mergers leave the secondary black hole wandering on a peripheral orbit at ~ 1 kpc away from the central, primary black hole. The naked black hole will then sink by dynamical friction on a longer timescale (Callegari et al. 2009, 2011; Khan et al. 2012a).

Higher-resolution simulations of disc galaxies have recently revealed the occurrence of additional features, indicating how rich is the outcome of mergers under different initial conditions. Van Wassenhove et al. (2014) have shown that, as the gas-rich merger

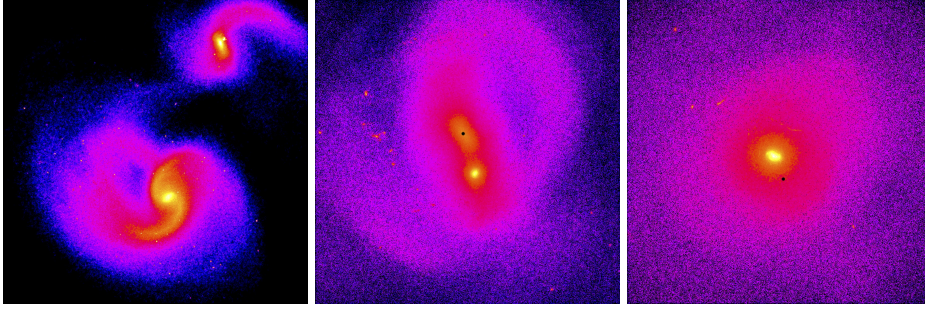


Fig. 5 Time sequence of stellar density snapshots in the 1:4 coplanar, prograde-prograde merger after the second peri-centre passage, at times 1.2, 1.43, and 1.48 Gyr, respectively. The scale of the left and central snapshots is 8 kpc, and 2 kpc for the right snapshot. A black dot marks the black hole in the primary galaxy nucleus which is dissolved during the interaction, while the secondary is at the centre of the highest density region of the secondary galaxy. In the last panel the secondary nucleus and black hole are near the centre of the mass distribution. Courtesy of Van Wassenhove et al. (2014).

progresses, the newly formed stellar nucleus of the less massive galaxy, denser on small scales, is able to dissolve the less concentrated nucleus of the primary, via impulsive tidal heating. This is illustrated in Figure 5 which shows how the denser nucleus of the secondary, at the end of the merger, finds itself in the midst of the mass distribution, having dissolved the nucleus of the main galaxy.

3.3 Black hole pairing in minor mergers: the role of mass accretion

Minor mergers among galaxies with mass ratios 1:10 or less show behaviours that are extremes, along the sequence of unequal-mass mergers, and may lead to wandering black holes, even in presence of a sizeable fraction of cold gas (Callegari et al. 2009, 2011). The fate of black holes in minor mergers depends not only on the gas content but on the orbital parameters, such as the degree of co-planarity, and in addition, on new input physics (neglected for seek of simplicity), i.e. accretion. During the encounter the secondary black hole as well as the primary can accrete from the surrounding gas and increase their mass. A mass increase can influence the dynamics of the secondary black hole, as a larger mass implies a more rapid sinking by dynamical friction. This correlation has been found in a number of simulations by Callegari et al. (2011) who showed that the black hole mass ratio q is not conserved during the merger. The secondary black hole is subjected to episodes of accretion which enhance the mass by an order of magnitude when interacting with the gas of the primary galaxy. Thus, the black hole mass ratio does not mirror that of the galaxies, and can be much higher than the initial value indicating that black holes in unequal-mass mergers may carry comparable masses at the time they form a close pair.

Figure 6 summarises these findings, i.e. the correlation between the ability of pairing (measured evaluating the black hole relative separation) and the mass ratio q , evaluated at the end of the simulation. Coplanar prograde mergers with higher fractions of gas lead to higher q and smaller black hole separations. Inclined mergers with large gas fractions can instead fail in bringing the black holes to a small separation. Torques acting on the satellite during the early phases of the merger are weaker for higher

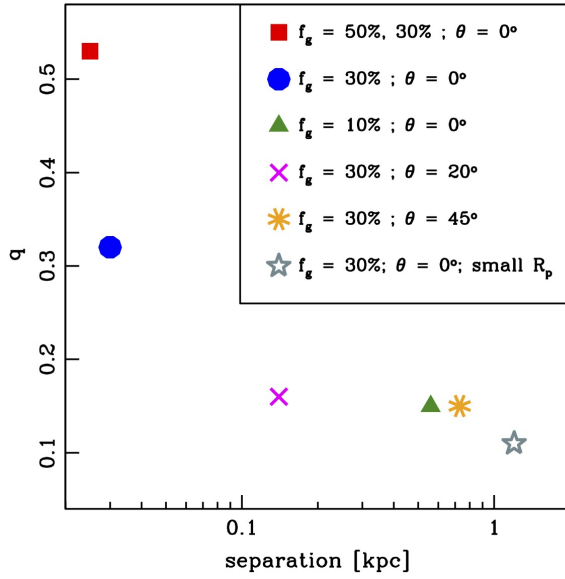


Fig. 6 Black hole mass ratio q versus relative separation, at the end of the simulation (when either a pair forms on the scale of the force resolution (10 pc), or the secondary black hole wanders at the periphery of the main galaxy), for the 1:10 mergers explored in (Callegari et al. 2011), labelled according to their initial gas fractions f_g , orbital inclination θ and initial peri-centre R_p . Courtesy of (Callegari et al. 2011).

inclinations, and for this reason the increase in mass ratio q during the first three orbits is milder than in the coplanar case with the same gas fraction. Moreover, a higher inclination corresponds to a slower orbital decay so that the satellite galaxy undergoes a larger number of tidal shocks before being disrupted, preventing further episodes of substantial accretion onto the secondary black hole. Finally, gas-rich mergers on closer orbits (i.e. with smaller peri-centre) are less effective in pairing contrary to what expected. Because of the smaller distance of approach and higher relative velocities between the satellite and the surroundings, ram pressure strips gas effectively, reducing the importance of the starburst that made the satellite less susceptible to stripping, and the accretion process onto the black hole. The joint action of these effects is therefore conducive to weak pairing, irrespective of the large amount of gas present initially.

In summary, minor mergers appear to fail in forming close black hole pairs in a number of cases, as the less massive galaxy is disrupted by tidal and ram pressure stripping at earlier times during the encounter so that dynamical friction is unable to deliver the secondary black hole to the centre of the main galaxy, within a Hubble time. The boundary between failure and success, i.e. between coalescence and wandering, is still poorly determined as it depends on the geometry, gas content and internal structure of the galaxies, and on the follow-up black hole dynamics on smaller scales (Khan et al. 2012a). Direct N -body simulations of gas-free minor mergers have shown that black hole coalescences can occur on timescales of one to a few Gyrs, regardless the mass ratio provided that its value $q \gtrsim q_{\text{crit}} \sim 0.05 - 0.1$ (Khan et al. 2012b). The rather abrupt transition at q_{crit} appears to result from the monotonic decrease of merger-induced triaxiality in the main galaxy with decreasing mass ratio. The secondary galaxy is too small and light to significantly perturb the massive primary, slowing down the rate of binary single star interactions and hardening. Judging from the results of simulations of galaxy minor mergers from a limited sample comprising gas-poor and gas-rich cases, a very rough boundary between coalescence and wandering appears to be at $q_{\text{crit}} \lesssim 0.1$.

Along parallel lines, N -Body/SPH cosmological simulations of massive disc galaxies, inclusive of black hole seed formation and growth, have shown that satellite galaxies containing black hole seeds are often tidally stripped as they merge with the primary while building the main galaxy disc. This creates naturally a population of wandering middleweight black holes in the massive spiral (from 5-10 wanderers), remnants of satellite cores (Bellovary et al. 2010).

4 Black hole dynamics in gaseous nuclear discs

SPH simulations of black hole dynamics in massive, rotationally supported nuclear discs represent a benchmark for studying the process of binary formation and coalescence, in gas-rich environments (Escala et al. 2005; Dotti et al. 2006, 2007, 2009; Fiacconi et al. 2013). These are *not ab initio* simulations, since the disc, in rotational equilibrium, is already in place as part of the remnant galaxy, or of the main galaxy, in case a minor merger has delivered the secondary black hole inside the disc of the massive host.

At present, there is no analytical model nor simulation that can trace the black hole dynamics in nuclear discs from the disc's periphery (at $\lesssim 100$ pc) down to the $\lesssim 10^{-3}$ pc scale (i.e. close and below a_{gw}) where gravitational waves drive the inspiral, due to the susceptibility of the gas to undergo gravitational instabilities conducive to star formation episodes and to the complexity of the gas thermodynamics in neutral and ionised media present on the smallest scales. In this context, key elements are the *rotation* of the underlying background, its *self-gravity*, the degree of *gas dissipation*, and the nature of *turbulence and viscosity*. Large scale gas discs can cool down, develop turbulence and inhomogeneities in the form of massive clumps which become sites of star formation. Gas can also dissipate the kinetic energy of the moving black holes via radiative cooling in a disc on smaller scales when the disc around the binary is nearly Keplerian. Thus, black hole inspiral in gaseous discs is mainly governed by processes of angular momentum exchange and radiative cooling. A compelling question to pose is whether angular momentum transport resulting from the gravitational interaction of the black holes with the gas is faster than that from the slingshot of stars.

In gaseous discs, we are led to distinguish three phases. There exists an early phase I-g of *nuclear-disc-driven migration* during which non axisymmetric perturbations in the density field excited by the gravitational field of the black hole(s) cause the braking of the orbit in regions where the disc dominates the gravitational potential (Escala et al. 2005; Dotti et al. 2006, 2007, 2009). The typical scale covered by I-g is between 100 pc down to ~ 0.1 pc.

With time, the gas mass enclosed in the orbit decreases below $m_{\bullet,t}$ and the black hole dynamics is dominated by their own gravitational potential. The binary then forms a Keplerian system. This corresponds to the onset of phase II-g of *binary-disc-driven migration*. In phase II-g, the tidal torques exerted by the binary on the disc are sufficiently intense to repel gas away from the binary clearing a cavity, called *gap* (Farris et al. 2014; Rafikov 2013; Hayasaki et al. 2013; D'Orazio et al. 2013; Roedig et al. 2012; Kocsis et al. 2012; Shi et al. 2012; Noble et al. 2012; Roedig et al. 2011; Cuadra et al. 2009; Hayasaki 2009; MacFadyen and Milosavljević 2008; Hayasaki et al. 2008, 2007; Ivanov et al. 1999; Gould and Rix 2000). The binary is then surrounded by a *circum-binary* disc. Rotation in the circum-binary disc is nearly Keplerian but the disc's structure is affected by the binary, acting as a source of angular momentum. In phase II-g, black holes migrate under the combined action of viscous and gravitational

torques which ultimately drive the binary into the third phase III of *gravitational-driven inspiral* where loss of orbital energy and angular momentum is due to the emission of gravitational waves. Not for all black hole masses this gas-assisted inspiral leads to coalescence in a Hubble time and more work is necessary along these lines (Cuadra et al. 2009).

Below, we explore phase I-g considering first a smooth nuclear disc and later a clumpy nuclear disc to study black hole migration on pc-scales. In a second step we will explore phase II-g when a circum-binary disc forms which controls the evolution of the binary on smaller scales.

4.1 Nuclear-disc-driven migration

4.1.1 Smooth circum-nuclear discs

In a number of targeted studies, the massive nuclear disc is described by a Mestel model: the disc, self-gravitating and axisymmetric, has rotation velocity V_{rot} independent of radius R . With constant V_{rot} , fluid elements in the disc are in differential rotation with $\Omega = V_{\text{rot}}/R$, and are distributed following a surface density profile $\Sigma(R) = \Sigma_d[R_d/R]$, where R_d is a scale radius. The disc mass within a radius R is then given by $M_{\text{Mestel}}(R) = M_d[R/R_d]$, with $M_d = 2\pi R_d^2 \Sigma_d$, and the circular velocity $V_{\text{rot}}^2 = GM_d/R_d$. The disc is pressure supported vertically, with aspect ratio h/R_d of $\sim 0.1 - 0.05$, and isothermal sound speed c_s such that the Toomre parameter Q is $\gtrsim 3$ everywhere, to prevent the development of gravitational instabilities. The disc is embedded in a more massive Plummer stellar sphere, representing the innermost region of the galactic bulge: hereon we refer to this configuration as circum-nuclear disc (Escala et al. 2005; Dotti et al. 2006, 2007, 2009).

In this smooth background (guaranteed by the large Q) one can trace the black hole dynamics, assuming a primary black hole of mass $m_{\bullet,1}$ at rest in the centre of the circum-nuclear disc, and a secondary black hole of mass $m_{\bullet,2}$ initially moving on a wide eccentric co-planar orbit inside the disc. The mass ratio q , the initial binary orbital elements, and the disc mass M_{Mestel} enclosed in the binary orbit (in excess of the binary mass $m_{\bullet,t}$, in the simulated volume), are free parameters to mimic different encounter geometries and mergers of galaxies with different stellar/gas mass contents.

Assisted by a series of N -Body/SPH simulations, these studies have highlighted key differences in the black hole dynamics compared to that in spherical collisionless backgrounds, the most remarkable being the dragging of the moving black hole into a co-planar co-rotating orbit with null eccentricity before the black holes form a binary (Dotti et al. 2006, 2007, 2009).

The simulations show that any orbit with large initial eccentricity is forced into circular rotation in the disc. In the different panels of Figure 7, we show the overdensity excited by the black hole along the orbital phase, for an initial value of the eccentricity e_0 equal to 0.9. The wake, that in a uniform medium, trails the motion of the perturber maintaining its shape, here changes both orientation and shape, due to the differential rotation of the underlying disc. The wake is trailing behind when the black hole is at pericentre, but is leading ahead when at apocentre, since there, the black hole is moving more slowly than the background, and this causes a temporary acceleration on $m_{\bullet,2}$. It is important to remark that this is a rapid change of e occurring on few orbital times. Circularisation is a fast process, and it is faster the cooler is the disc,

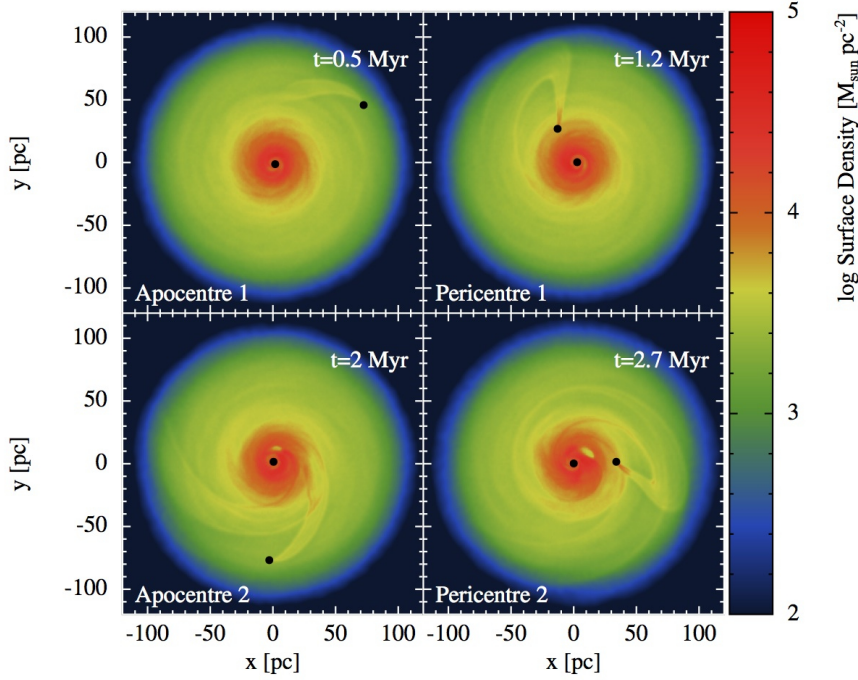


Fig. 7 Colour-coded gas surface density of a smooth disc of mass $M_d = 5 \times 10^8 M_\odot$, for a black hole binary with $q = 0.1$ and a primary black hole of $10^7 M_\odot$. The initial eccentricity is $e_0 = 0.7$. Snapshots refer to four different times, covering the process of circularisation lasting a few Myrs. The gas and the secondary black hole rotate counter-clockwise. The position of the black holes is marked by black dots. In the top and bottom left (right) panels the density wake excited by the secondary black hole is leading (trailing) the orbit, resulting in the circularisation of the relative orbit. Courtesy of D. Fiacconi.

i.e. the denser is the disc. Sinking times are found to depend on the equation of state adopted, i.e on the polytropic index γ used to model the thermodynamic behaviour of the gas.

A further signature of a rotating background is the *angular momentum flip* of an initially counter-rotating orbit, if it exists (Dotti et al. 2009).³ Initially, the gas opposes to the motion of the black hole as the density perturbation is always in the form of a trailing wake which causes an effective brake. The change of the orbital angular momentum from negative to nearly null values is further facilitated by the fact that, while the orbit decays, the black hole interacts with progressively denser regions of the disc. The orbit is nearly radial when the orbital angular momentum changes sign but the change is so rapid, relative to the orbital time, that the black hole is forced to co-rotate. When co-rotation establishes along an eccentric orbit, the orbital momentum increases under the circularising action of dynamical friction (non axisymmetric wake) in its co-rotating mode. Thus, a further prediction of black hole inspiral in rotating discs is that gas-dynamical friction conspires to turn counter-rotating orbits into co-rotating ones, even before the formation of a Keplerian binary.

³ This is a possibility that may occur in the case of a minor merger where the incoming black hole in the satellite galaxy enters the main galaxy from a co-planar counter-rotating orbit.

After circularisation, the secondary black hole continues to spiral in as it experiences a net negative torque, despite having reduced its relative velocity with respect to neighbouring fluid elements.⁴ Dynamical friction is a non-local process and in a disc there is a residual velocity difference between the black hole and the more distant rotating fluid elements. One can view the migration process described in the text again as a manifestation of the larger scale gravitational perturbation excited by the black hole, but this time the drag is inside a rotating inhomogeneous background. The net torque results from the sum of positive (inside the black hole orbit) and negative (outside) contributions as the perturbation is highly non axisymmetric due to differential rotation. The black hole $m_{\bullet,2}$ is able to excite a non axisymmetric perturbation in the disc structure which produces a net negative torque on $m_{\bullet,2}$. This process is reminiscent to Type I planet migration, but with key differences. While in planet migration, the central star dominates the gravitational potential and the disc's self-gravity is negligible, in disc-driven black hole migration (phase I-g) the disc is dominant, while the gravity of the central black hole is negligible. In Type I migration, the net torque on the planet is the sum of the Lindblad and co-rotating resonances, computed in the linear perturbation theory under the hypothesis that the planet migrates on a timescale much longer than the orbital time, so that the small-amplitude perturbation is periodic in the disc frame. By contrast, during phase I-g of black hole migration, the torque on the secondary black hole comes from the non-linear density perturbations that $m_{\bullet,2}$ excites in the disc. Figure 8 shows the fast orbital decay that the secondary black hole experiences after circularisation (Fiacconi et al. 2013).

To gain some insight into nuclear-driven-disc migration in a Mestel disc, we estimate the migration time following a simple argument to capture key dependences of τ_{mig} on the disc properties and black hole mass (Armitage 2013). In the two-body approximation, a fluid particle, approaching $m_{\bullet,2}$ along a straight-line with impact parameter b and relative velocity $v_{\text{rel}} \sim a\delta\Omega \sim b\Omega$ experiences a velocity change parallel to \mathbf{v}_{rel} of the order of $\delta v_{\parallel} \sim 2G^2 m_{\bullet,2}^2 / (b^2 v_{\text{rel}}^3)$, where a denotes the black hole distance from the centre of the disc. As gas exterior to the secondary black hole moves more slowly than the black hole in the disc, it gains velocity parallel to \mathbf{v}_{rel} increasing its angular momentum. As angular momentum is conserved, this implies a *decrease* in the angular momentum per unit gas mass for the black hole equal to $\sim -a\delta v_{\parallel}$. Note that gas interior to the black hole orbit exerts a torque of opposite sign, so that the net torque depends on a delicate balance. As simulations show inward migration and larger torques in the black hole vicinity, we compute the rate of change of angular momentum considering only neighbouring gas particles in the trailing side of the spiral density perturbation, contained in a cylinder of scale height $b \sim h$. Accordingly, the mass flux on $m_{\bullet,2}$ is $\delta m / \delta t \sim 2\pi h \Sigma v_{\text{rel}} \sim 2\pi h^2 \Sigma \Omega$, where Σ and Ω are evaluated at a . The resulting torque on the black hole can thus be written as $T_1^{\text{Mestel}} \sim -4\pi\zeta [m_{\bullet,2}/M_{\text{Mestel}}(a)]^2 \Sigma a^4 \Omega^2$, where $\zeta = \zeta'(a/h)^3$ brackets uncertainties in the normalisation of the torque and its dependence on the aspect ra-

⁴ In a uniform, isotropic gaseous background, gas-dynamical friction vanishes when the velocity of the perturber falls below the sound speed (Ostriker 1999). Kim et al. (2008) extend the work by Ostriker (1999) considering double perturbers moving on a circular orbit in a homogeneous gaseous medium. They find that the circular orbit makes the wake of each perturber asymmetric, creating an over-dense tail at the trailing side. The tail not only drags the perturber backward but it also exerts a positive torque on the companion. This finding shows that the orbital decay of a perturber in a double system, especially in the subsonic regime, can take considerably longer than in isolation.

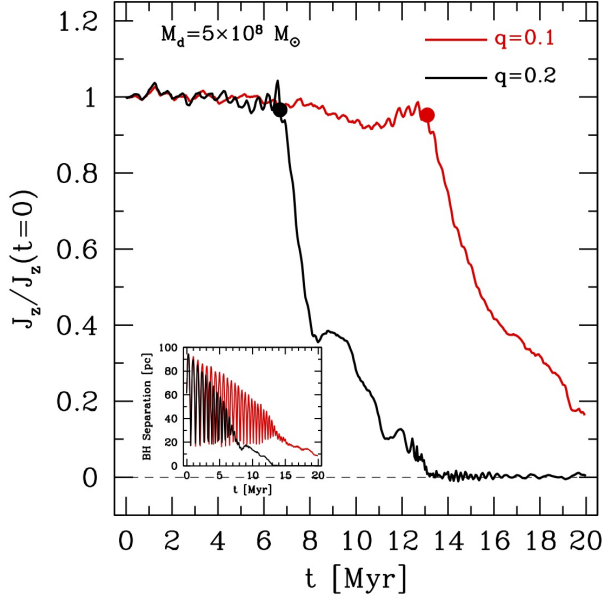


Fig. 8 The evolution of the angular momentum of the secondary black hole orbiting inside a smooth circum-nuclear disc of mass $M_d = 5 \times 10^8 M_\odot$. The initial eccentricity is $e_0 = 0.9$. Red and black colours refer to $q = 0.1$ and $q = 0.2$, respectively ($m_{\bullet,1} = 10^7 \text{ sun}$ in the runs). The dot marks the time at which the circularisation of the orbit by dynamical friction is completed. The inset shows the black hole separation (in pc) versus time (in Myr). At circularisation, $M_{\text{Mestel}}(a)/m_{\bullet,2} \sim 150$ and 75 for the two cases, respectively. Courtesy of D. Fiacconi.

tio. As in a Mestel disc the circular velocity is independent of radius a , the black hole sinks from an initial radius a_i to a much smaller radius a_f on a migration time scale $\tau_{\text{mig,Mestel}}^I \sim C \Omega_i^{-1} [M_{\text{Mestel}}(a_i)/m_{\bullet,2}]$, where $C = (h/a)^3/(4\zeta')$.⁵ We remark that the scaling of $\tau_{\text{mig,Mestel}}^I$ with the disc and black hole mass holds true provided $M_{\text{Mestel}}(a) > m_{\bullet,1} > m_{\bullet,2}$.

Nuclear discs, stable against fragmentation, are nevertheless ideal. The gas can not be treated as a simple one-phase fluid. Galactic discs are sites of local gravitational instabilities conducive to star formation episodes: massive stars inject energy in the form of winds and supernova blast waves, feeding back energy into the disc and the gas is multi-phase, and clumpy. Thus, it is of importance to understand how the black hole sinking is affected by the inhomogeneous substructure of star forming discs. To this aim, in the next subsection, we explore black hole dynamics in clumpy discs.

4.1.2 Clumpy circum-nuclear discs and stochastic orbital decay

In real astrophysical discs, massive gas clouds coexist with warmer phases and a polytropic equation of state, often used in SPH simulations, provides only an averaged representation of the real thermodynamical state. Cold self-gravitating discs are unstable to fragmentation and attain stability when stars, resulting from the collapse and/or collision of clouds, inject energy in the form of winds and supernova blast waves, feeding back energy into the disc now composed of stars and a multiphase gas.

⁵ The coefficient ζ can be inferred from dedicated numerical experiments. In the case explored, the coefficient $\zeta' \sim 0.04$, to match the sinking time with a simulation. A systematic analysis is necessary to estimate ζ' in a Mestel disc (paper in preparation). Furthermore, the scaling of $\tau_{\text{mig,Mestel}}^I$ with the aspect ratio h/a can not be derived from this elementary argument, as discussed in Armitage (2013).

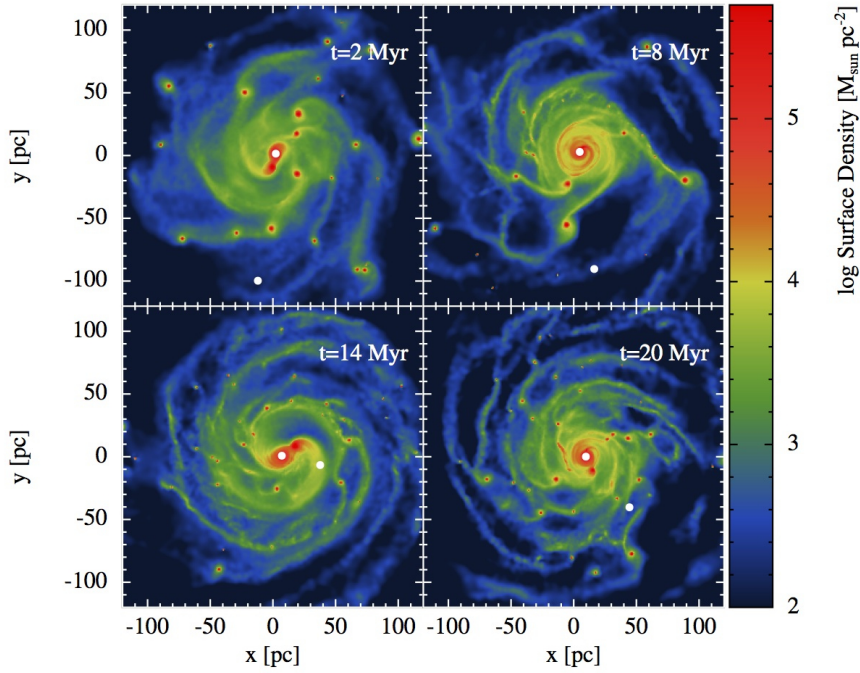


Fig. 9 Colour-coded face-on view of the gas surface density of a clumpy disc model with $M_d = 5 \times 10^8 M_\odot$, $m_{\bullet,1} = 10^7 M_\odot$, $q = 0.1$ and initial eccentricity $e = 0.7$, plotted at four different times. The position of the black holes is marked by white dots. Courtesy of D. Fiacconi.

Due to the complexity of implementing this rich physics at the required level of accuracy, a first step ahead is to insert a phenomenological cooling prescription to allow the formation of clumps in a controlled way (Fiacconi et al. 2013). Clumps of size ~ 5 pc in the mass interval between $10^5 M_\odot$ and $10^7 M_\odot$ develop in the disc, and evolve as they mass segregate, collide with each other and interact with the secondary black hole. Acting as massive perturbers, they disturb the otherwise smooth black hole orbital decay due to the stochastic behaviour of their torques that are not coherent in time. Several close encounters between $m_{\bullet,2}$ and the massive clumps act as gravitational slingshots, causing an impulsive exchange of orbital energy and angular momentum. Thus, the black hole deviates from its original trajectory either outwards, or inwards or out of the disc plane (above the typical scale height of the disc). When moving on an inclined orbit the black hole experiences the weaker dynamical friction of the stellar background, resulting in a longer orbital decay timescale. The secondary black hole can also be captured by a massive clump forming a pair which segregates rapidly toward the centre. Figure 9 shows the evolution of the gas surface density of a selected run, and the position of the two black holes (marked as white dots) at four different times.

The *stochastic* behaviour of the black hole orbit, resulting from the incoherence of torques, emerges mainly when the clump to black hole mass ratio is $M_{\text{clump}}/m_{\bullet,2} \gtrsim 1$. This enlarges the values of the decay time which now range from less than $\lesssim 1$ up to $\gtrsim 50$ Myr. This suggests that describing the cold clumpy phase of the interstellar medium in nuclear discs, albeit so far neglected, is important to predict the black hole

dynamics. Ongoing simulations in a multi-phase star forming nuclear disc resulting from the collision of two discs following a merger produce results that are intermediate between the smooth and clumpy case (Lupi et al. in preparation).

4.2 Binary-disc-driven migration

In Section 4.1.1 we followed the black hole inspiral during phase I-g, in presence of a self-gravitating, rotationally supported disc much heavier than the binary, a condition leading to migration as described in (Escala et al. 2005; Dotti et al. 2006, 2007, 2009). However, with binary decay, the disc mass M_{Mestel} enclosed in the black hole orbit a decreases with time falling below $m_{\bullet,t}$. The black holes then form a Keplerian binary surrounded by a less massive disc, called *circum-binary* disc, dominated by the gravity of the binary and its quadrupolar field.

If we impose continuity in the physical processes, there might exist an intermediate phase whereby migration of the secondary black hole is controlled by *resonant* torques. In close resemblance to Type I planet migration, and for very small binary mass ratios $q \ll 1$, the resulting torque on $m_{\bullet,2}$ is $T_{\text{I}}^{\text{mig,Kep}} = -\zeta_K [m_{\bullet,2}/m_{\bullet,1}]^2 \Sigma a^4 \Omega_K^2$, where Ω_K is the Keplerian rotational velocity in the gravitational field of $m_{\bullet,1}$ evaluated in a , Σ the disc surface density in the immediate vicinity of $m_{\bullet,2}$, $\zeta_K = (1.36 + 0.54\alpha)(a/h)^2$, and α the slope of the surface density profile $\Sigma \propto a^{-\alpha}$ of the underlying Keplerian disc (Tanaka et al. 2002; Armitage 2013). Notice that because of the natural scaling present in the problem, the torque $T_{\text{I}}^{\text{Kep}}$ differs from the expression of $T_{\text{I}}^{\text{Mestel}}$ having $m_{\bullet,1}$ in place of $M_{\text{Mestel}}(a)$ as reference mass for the gravitational potential. In this case, the migration time reads as $\tau_{\text{mig,Kep}}^{\text{I}} \propto [m_{\bullet,1}/m_{\bullet,2}][m_{\bullet,1}/M_{\text{disc}}(a)]\Omega_K^{-1}$, under the condition that the disc mass enclosed in the black hole orbit $M_{\text{disc}}(a) < m_{\bullet,1}$.

As described in Section 3, black hole binaries form preferentially in the aftermath of major mergers so that the binary mass ratio $q \lesssim 1$. Furthermore, accretion drives q to larger and larger values, in the case of minor mergers under specific circumstances (Callegari et al. 2011). Thus, it is quite likely that migration under the action of torques excited by resonances is a missing step, in the dynamical evolution of black hole binaries. At this time the binary is expected to alter profoundly the structure of the underlying disc.

Thus, a key question poses: will the black holes sink down to the domain of gravitational wave inspiral transferring their angular momentum to the disc, or would the binary stall? Is there a phase II-g of migration and under which conditions? This phase is in fact somewhat controversial, as the black hole fate depends on whether the disc is a one-time, short-lived excretion disc (Lodato et al. 2009; Pringle 1991), or an extended long-lived disc (Rafikov 2013). These are conditions that are not recoverable from realistic larger-scale simulations as it is difficult to model the transition from a disc dominated by self-gravity and gravito-turbulence to a disc dominated by magneto-hydrodynamical turbulence stirred by magneto-rotational instabilities in the conducting fluid (Shi et al. 2012).

Unless the binary is surrounded by a geometrically thick disc or envelope and decays promptly (del Valle and Escala 2012, 2014), the tidal force exerted by the binary on the circum-binary disc is expected to eventually clear a cavity. The picture is that the binary transfers orbital angular momentum to the disc by exciting non-axisymmetric density perturbations in the disc body, causing the formation of a low-density, hollow region, called *gap* (Farris et al. 2014; Rafikov 2013; Hayasaki et al. 2013; Roedig et al.

2012; Kocsis et al. 2012; Shi et al. 2012; Roedig et al. 2011; Cuadra et al. 2009; Hayasaki 2009; Haiman et al. 2009; MacFadyen and Milosavljević 2008; Hayasaki et al. 2008, 2007; Ivanov et al. 1999; Gould and Rix 2000; Pringle 1991). Viscous torques in the disc oppose gas clearing by the tidal field of the binary and ensure strong binary-disc coupling. Under these conditions, the binary enters a regime of slow orbital decay [referred to as Type II migration in the case of planets (Artymowicz and Lubow 1994, 1996; Gould and Rix 2000; Armitage and Natarajan 2002; Armitage 2013)] during which the inner edge of the circum-binary disc compresses in coordination with the hardening of the binary, so that the size $\delta(t)$ of the gap decays remaining close to twice the binary semi-major axis, $\delta \sim 2a(t)$.

Due to the tidal barrier offered by the binary, gas piles up at the inner rim of the disc. One can view the binary as acting as a dam, halting the gas inflow. Accordingly, the accretion rate in the circum-binary disc is not constant in radius and no strict steady state is ever attained in the disc body. In 1D modelling of circum-binary discs, the disc is seen to evolve into a state of constant angular momentum flux (Rafikov 2013), and binary decay leads to a secular and self-similar evolution of the disc as first suggested in (Ivanov et al. 1999). This happens when the system loses memory of the natural scale a , set by the size of the cavity and binary orbit, soon after the angular momentum injected by the binary has been transmitted to the larger scale extended disc (Rafikov 2013). Gap opening implies longer hardening time scales compared to nuclear-disc-driven migration, now controlled by the viscous time at the inner disc edge.

The migration time can be estimated as $\tau_{\text{mig}}^{\text{II}} \sim \tau_{\nu}[(m_{\bullet,2} + M_{\text{d}}^{\text{edge}})/M_{\text{d}}^{\text{edge}}]$ where $M_{\text{d}}^{\text{edge}} \sim \Sigma(R)R^2$ is the local mass near the inner edge of the disc, at $R \sim 2a-3a$ where the surface density has a peak, and τ_{ν} the disc viscous time there: $\tau_{\nu} \sim (2/3)R^2/\nu \sim 2\pi R^2 \Sigma/\dot{M}$ where $\dot{M} \sim 3\pi\nu\Sigma$ is the mass accretion rate in an unperturbed reference disc (Shakura and Sunyaev 1973). When $M_{\text{d}}^{\text{edge}} > m_{\bullet,2}$, the secondary black hole behaves as a parcel in the viscous disc and migrates on the viscous timescale, whereas when $M_{\text{d}}^{\text{edge}} < m_{\bullet,2}$ migration slows down and occurs on a timescale longer than τ_{ν} . Condition $M_{\text{d}}^{\text{edge}} < m_{\bullet,2}$ is often referred to as secondary-dominated Type II migration (Haiman et al. 2009; Syer and Clarke 1995). The opposite regime is referred to as disc-dominated Type II migration.

The timescale $\tau_{\text{mig}}^{\text{II}}$ can be recovered if one assumes a torque on the binary of the form $T_{\text{II}}^{\text{mig}} \sim -\xi j_o \dot{M} \sim \xi' j_o M_{\text{d}}^{\text{edge}} \Omega_K$ where $j_o = (\mu/m_{\bullet,t})(Gm_{\bullet,t}a)^{1/2}$ is the binary angular momentum per unit mass, and ξ or ξ' determined by numerical simulations, e.g. (MacFadyen and Milosavljević 2008; Roedig et al. 2012; Shi et al. 2012). The above expression for the torque relates the rate of binary orbital decay to the local disc mass $M_{\text{d}}^{\text{edge}}$ near the inner edge of the disc. Therefore, depending on how $M_{\text{d}}^{\text{edge}}$ varies over the relevant timescales, i.e. whether the disc is continuously re-filled of gas to keep $M_{\text{d}}^{\text{edge}}$ nearly stationary, or the disc mass is consumed before the binary has evolved substantially, orbital decay accelerates or decelerates, returning the problem to the old, outstanding issue on whether black holes are continuously fed in galactic nuclei or not, and on which timescale.

Semi-analytical expressions of the migration time have been derived in (Haiman et al. 2009) considering orbital decay within a Shakura & Sunyaev accretion disc (Shakura and Sunyaev 1973). This enabled the authors to evaluate the disc surface density, opacity, viscosity and ultimately $M_{\text{d}}^{\text{edge}}$ as the binary transits through the outer/middle and inner zones of the disc. Under these simplifying assumptions (of a

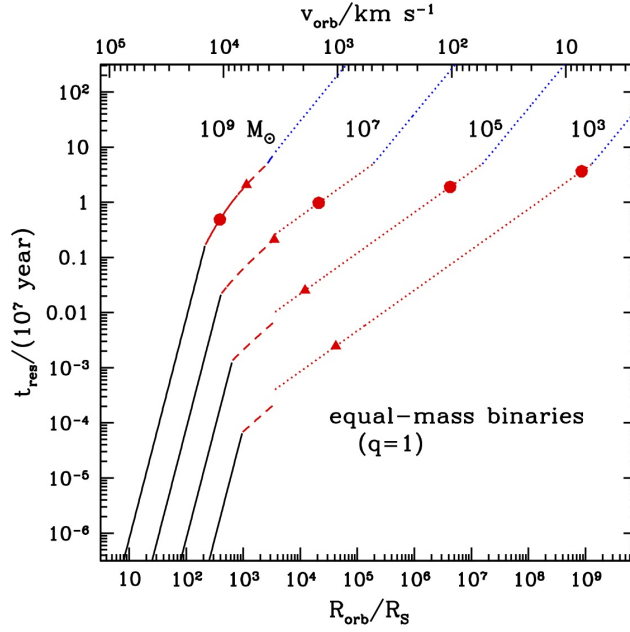


Fig. 10 Residence time $|a/\dot{a}|$ of equal-mass black hole binaries, embedded in a steady circum-binary disc, as a function of the black hole separation (in units of $2Gm_{\bullet,t}/c^2$), as computed in (Haiman et al. 2009) for a reference disc model. The top x -axis label refers to the Keplerian relative orbital velocity of the black holes in the binaries. The four curves correspond to binaries with total masses of $m_{\bullet,t} = 10^3, 10^5, 10^7$ and $10^9 M_{\odot}$ as labeled. The large dots denote the critical radius beyond which the assumed circum-binary Keplerian disc is unstable to fragmentation. Similarly, triangles denote radii beyond which the disc may be susceptible to ionisation instabilities (the gas temperature falls below 10^4 K). In each case, blue/red colors indicate whether the disc mass enclosed within the binaries orbit is larger/smaller than the black hole mass $m_{\bullet,2}$. The dotted/dashed/solid portion of each curve indicates the outer/middle/inner disc region. Note that in the disc-dominated regime (blue segments) the binary residence time is $\sim 10^9$ yrs, while it decreases below $\sim 10^7$ yrs for all binaries, i.e. independent of their mass, at the entrance in the stable region of a circum-binary disc (red dots). Courtesy of Haiman et al. (2009).

steady 1D disc), Haiman et al. (2009) have shown that the sinking time of the binary is a *monotonic decreasing function of the binary orbital period* (or separation). The residence time $t_{\text{res}} \sim |a/\dot{a}|$ for equal-mass binaries (which is in this context close to $\tau_{\text{mig}}^{\text{II}}$) is plotted in Figure 10 from Haiman et al. (2009) for a disc with α viscosity parameter equal to 0.3, a radiative efficiency of 0.1 and an accretion rate equal to 0.1 of the Eddington value. In the disc-dominated regime when $M_{\text{d}}^{\text{edge}} > m_{\bullet,2}$ the migration timescale is of the order of $\sim \text{Gyr}$ and when $M_{\text{d}}^{\text{edge}} < m_{\bullet,2}$ it drops below 10^7 yrs, showing weak dependence of the binary mass. Similar timescales have also been found in Rafikov (2013) when considering 1D disc models undergoing self-similar evolution [see also figure 6 of Haiman et al. (2009)]. Despite these studies, we are nonetheless

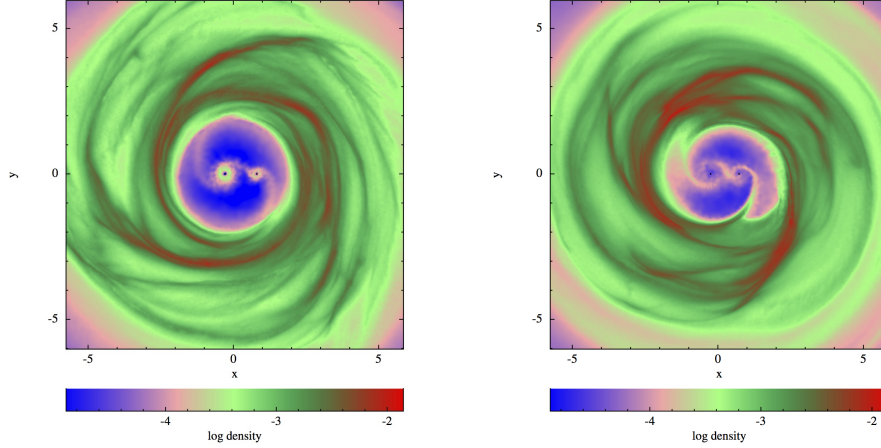


Fig. 11 Color-coded gas surface density of two Newtonian, self-gravitating circum-binary discs, showing the presence of a binary region with the two black holes and their mini-discs, a porous cavity filled with streams, the inner rim or edge working as a dam, and the body disc. Left (right) panel refers to a run with gas in the cavity treated with an isothermal (adiabatic) equation of state. Courtesy of Roedig et al. (2012).

far from having a reliable estimate of the migration timescale in circum-binary discs under a variety of conditions, given the rich physics involved.⁶

Gap opening and/or maintenance of the inner cavity around massive black holes have been seen in numerous numerical simulations of both Keplerian and self-gravitating circum-binary discs (MacFadyen and Milosavljević 2008; Shi et al. 2012; Cuadra et al. 2009; Roedig et al. 2011; del Valle and Escala 2012). But interestingly, recent 2D and 3D simulations have demonstrated that the binary+disc system contains as many as three discs and that these discs may persist being constantly fed by gas flowing through the gap. The three discs comprise the circum-binary disc plus two mini-discs around each member of the binary (Farris et al. 2014; Shi et al. 2012; Roedig et al. 2012, 2011). This is due to the fact that the disc inner edge is porous (for sufficiently high disc aspect ratios): high velocity, narrow streams of gas leak periodically through the dam into the inner cavity, modulated by the binary orbit (Roedig et al. 2012; Shi et al. 2012; Noble et al. 2012; D’Orazio et al. 2013; Farris et al. 2014).

Figure 11 shows the distribution of gas around the black hole binary after gap formation, from two SPH-3D simulations of Newtonian, massive circum-binary discs

⁶ As an example, in recent studies of planet migration by Duffell et al. (2014) it has been shown, using highly accurate numerical calculations, that the actual migration rate is dependent on disc and planet parameters, and can be significantly larger or smaller than the viscous drift rate τ_ν^{-1} . In the case of disc-dominated migration the rate saturates to a constant value which is in excess of the viscous rate while in the opposite regime of a low-mass disc, the migration rate decreases linearly with disc mass.

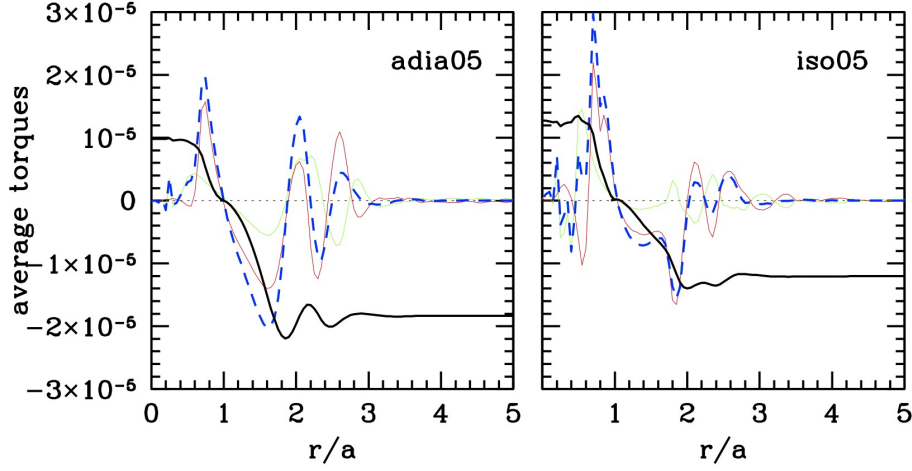


Fig. 12 Differential torques dT/dR and integrated torque T (averaged over the time span of the simulation, and in code units) exerted by the disc on the binary with mass ratio $q = 0.1$ as a function of the radial distance, in units of the binary separation a , for the adiabatic (left) and isothermal (right) run from (Roedig et al. 2012). In each panel, the differential torque acting on the primary is plotted in green, on the secondary in red, and the sum of the two in blue. Notice that the torque density dT/dR shows different signs and starts oscillating around the zero point at distances far from the binary where the binary-disc coupling decreases sharply. The black line refers to the integrated torque T up to a distance R : T is positive inside a , and negative outside giving a total negative contribution. Courtesy of Roedig et al. (2012).

(Roedig et al. 2012) which differ from one another due to a different thermodynamic modelling of the gaseous streams in the cavity: isothermal (on the right side) and adiabatic (on the left side). The figure highlights the occurrence of different domains in the disc (from outside in): the *disc body* $R > 2.5a$ where spiral patterns develop; the *cavity edge*, at radii $2 < R < 2.5a$, which is porous and leaky; the *cavity region* or gap, between $a < R < 2a$, which is almost devoid of gas except for the presence of tenuous streams; the *binary* region, at $0 < R < a$, with the two black holes and their mini-discs, fed by gas from the disc body flowing through the cavity across the porous dam. The mini-discs and the cavity are sharper in the isothermal case compared to the adiabatic case where the amount of gas impacting the gap is larger. Only a fraction of this gas is captured by the black holes to form the mini-discs, the remaining being swiftly ejected away. The different regions highlighted in Figure 11 contribute to the differential torque dT/dR on the binary with different signs as illustrated in Figure 12, for the case of a Newtonian self-gravitating disc (in the adiabatic and isothermal model, respectively). One can notice that the differential torque shows an oscillatory behaviour with a sharp maximum at the location of the secondary black hole ($R \sim 0.75a$), and

a deep minimum in the cavity region. Positive and negative peaks alternate in the disc body that almost cancel out, giving a negligible contribution to the total torque. Torques on the secondary black hole are always larger than on the primary, due to its proximity to the inner rim of the disc, resulting in a stronger interaction.

In summary, simulations now indicate that clearing a cavity in the disc does not prevent the inflow of gas through streams across the cavity's edge. Thus accretion of a fraction of this gas on the black holes, and preferentially onto the secondary (nearer to the disc's edge) may be a persistent feature (Farris et al. 2014). Thus binary evolution becomes more complex than outlined in the first part of this section. All binary elements evolve over time and in some cases inward migration can turn into outward migration (Hayasaki 2009; Roedig et al. 2012). The evolution equation for the semi-major axis of a binary depends on changes in the eccentricity, mass, reduced mass and on the exchange of angular momentum between the binary and the three discs through a generalised T . All these contribute to $\dot{a}/a = 2T/J_\bullet - \dot{m}_{\bullet,t}/m_{\bullet,t} - 2\dot{\mu}/\mu + 2e\dot{e}/(1-e^2)$ where J_\bullet is the binary angular momentum. The sign of this derivative thus depends on different effects.

The binary eccentricity tends to increase during the binary-disc coupling (Armitage and Natarajan 2005; MacFadyen and Milosavljević 2008), and the growth of e has also been seen in 3D numerical simulations (Roedig et al. 2011). Progress in the analysis of this process has revealed that such excitation can not grow indefinitely, as *saturation* occurs due to the interaction of the secondary black hole with gas near the inner rim of the disc body, and to the accumulation of gas around the black holes in the mini-discs (Roedig et al. 2011). The initial rise of e can be understood, as in Section 4.1.1, using dynamical friction in a differentially rotating background as leading argument. The secondary black hole, closer to the circum-binary disc, induces a trailing density wave near the inner rim which reduce its tangential velocity, causing a loss of orbital angular momentum. The eccentricity e grows and continues to grow as long as the gas at the inner edge of the circum-binary disc moves with a lower angular velocity. However the progressive decay of the black hole tangential velocity with increasing e leads eventually to a reversal of the sign of the relative velocities, the gas moving faster than the black holes, thus developing a wake heading in front which leads to an acceleration of the black hole. The process reaches saturation, and this is found to occur about $e \sim 0.6 - 0.8$. Furthermore, when the binary becomes very eccentric, the secondary, less massive black hole passes through the mini-disc of the primary suffering a deceleration at peri-centre which in turn decreases e , which then attains a saturation value.

The mass of the two black holes tend to increase as well, and the increase of the mass of the secondary black hole is even higher, being closer to the disc, thus driving q toward unity (Farris et al. 2014). The mass accretion rate is not severely limited (compared to the case of a single isolated black hole) and \dot{M} is found to be modulated at the binary orbital period and higher harmonics (Farris et al. 2014; Roedig et al. 2011). Interestingly, modulated accretion suggests a promising avenue for producing a modulated electromagnetic signal permitting the identification of binaries during migration in circum-binary discs at different orbital phases along the path to coalescence (Eracleous et al. 2011; Decarli et al. 2013; Montuori et al. 2012).

5 Timescales: an overview

Galaxy interactions and mergers are the sites of formation of dual, binary, coalescing and recoiling black holes. Associated to these different dynamical phases there is a zoo of sources: the dual, binary and recoiling AGN if the black holes are active. A residence time is associated to each phase: in phase I, the dynamical friction timescale τ_{df} or /and the dynamical friction timescale which accounts for tidal mass loss $\tau_{\text{df,tidal}}$; in phase II, the hardening time in a stellar background τ_{Hard} (which falls in the interval between τ_{hard}^* and τ_{rel}), or/and (in gas-rich mergers) the timescale of nuclear-disc-driven migration $\tau_{\text{mig,Mestel}}^{\text{I}}$ and binary-disc-driven migration $\tau_{\text{mig}}^{\text{II}}$; ultimately in phase III, the gravitational wave timescale τ_{gw} .

There is no simple recipe to calculate the residence times in terms of fundamental parameters such as the black hole mass and mass ratio since these timescales depend on the morphology of the interacting galaxies, the geometry of the encounter, the gas fraction, and most importantly on the complex input physics of difficult implementation even in current state-of-the-art simulations.

The characteristic coalescence time τ_{coal} would be the sum of the timescales associated to the different phases (I, II or I-g,II-g, and III), calculated along each individual pathway. Their value depends, even in the minimal model, on whether the merger is gas-poor (dry) or gas-rich (wet), and major or minor. As no unique pathway exists for a pair, τ_{coal} can be estimated simply considering the maximum of all residence times. This timescale should then be compared with the Hubble time or better with the running age of the universe at the time of coalescence, given that eLISA sources are typically at high redshifts (Amaro-Seoane et al. 2013).

Here is a tentative summary of the timescales inferred from the whole body of works, in the black hole mass range $\lesssim 10^7 M_{\odot}$ and for values of the initial black hole mass ratio q (which indicates the mass ratio between the two interacting galaxies). If the "zero" time is calculated when the merger of the baryonic components (bulge and disc) is completed, i.e. when the black holes behave as individual objects moving in the relic galaxy, the relevant timescales in different environments and conditions are expected to cluster approximately around these values:

- In dry major mergers ($q > q_{\text{crit}} \sim 0.1$): (i) dynamical friction time $\tau_{\text{df}} \lesssim [10 \text{ Myr} - 100 \text{ Myr}]$ (Yu 2002) – (ii) hardening timescale $\tau_{\text{Hard}} \sim 1 \text{ Gyr}$ to a few Gyr (Khan et al. 2011).
- In wet major mergers ($q > q_{\text{crit}} \sim 0.1$): (i) gas-dynamical friction time $\tau_{\text{df}} \lesssim [10 \text{ Myr} - 100 \text{ Myr}]$ (Mayer et al. 2007; Chapon et al. 2013; Roškar et al. 2014) – (ii) nuclear-disc-driven migration time $\tau_{\text{mig,Mestel}}^{\text{I}} \sim (5 \text{ Myr} - 50 \text{ Myr})$ (Escala et al. 2005; Dotti et al. 2006, 2007, 2009; Fiacconi et al. 2013) – (iii) binary-disc-driven migration $\tau_{\text{mig}}^{\text{II}} \sim 10 \text{ Myr}$ (Haiman et al. 2009).
- In dry minor mergers ($q < q_{\text{crit}} \sim 0.1$): (i) dynamical friction time $\tau_{\text{df,tidal}} \lesssim [10 \text{ Myr} - 100 \text{ Myr}]$ (Yu 2002) – (ii) hardening timescale $\tau_{\text{Hard}} \sim 1 \text{ Gyr}$ up to a few Gyr (Yu 2002; Khan et al. 2012b).
- In wet minor mergers ($q < q_{\text{crit}} \sim 0.1$): (i) dynamical friction time with corrections due to tidal stripping $\tau_{\text{df,tidal}} \lesssim 100 \text{ Myr}$ or wandering (Callegari et al. 2009, 2011). The fate is uncertain. Depending on the geometry of the encounter and gas fraction, the secondary black hole may wander in the primary galaxy.

6 Summary and future prospects

The study of the dynamics of black holes, with masses from $10^4 M_\odot$ up to $10^9 M_\odot$, inside galaxies displaying a large variety of morphologies and masses, is not a side problem: it is central if we want to search for or recognise signs of their duality and/or coalescence at electromagnetic level, and if we want to detect the gravitational waves emitted at the time of black hole coalescence. Observationally the search of dual AGN (accreting black holes in merging galaxies at separations of $\sim \text{kpc}$), and of binary (pc scales) and recoiling AGN have received attention in recent years (Eracleous et al. 2011; Liu et al. 2011; Komossa 2012; Koss et al. 2012; Liu et al. 2013; Decarli et al. 2013; Comerford and Greene 2014; Lusso et al. 2014; Liu et al. 2014). There has been some major advances in the study of the dynamics of black holes in merging galaxies, over the last years, and the points to remember and to take away for future reference are:

1. Black holes in binaries can reach coalescence under the emission of gravitational waves. But, for this to happen, the black holes have to be driven to separations as small as $\sim 10^{-3}$ pc or less, as gravity is a weak force and gravitational waves are a manifestation of the strong field regime (Sathyaprakash and Schutz 2009). This is a minuscule distance, compared to galaxy's sizes, and merging galaxies are the sites where these events can occur. Nature has thus to provide a series of mechanisms able to extract energy and angular momentum, from the large scale of the merger (at least a few kpc) to the micro-parsec scale, i.e. the scale at which the black hole horizons touch. The path to coalescence is long and complex, and stalling of the binary at some scale is a possibility.
2. Three phases accompany the path to coalescence: the pairing, hardening, and gravitational-wave driven inspiral phases. Stars or gas, or stars and gas drive the black hole inspiral, depending on whether galaxies are gas-rich or gas-poor. Bottlenecks can appear at various scales and a major effort is to identify possible obstacles. The last parsec problem, i.e. the stalling of a massive black hole binary at the centre of a large spherical collisionless galaxy was highlighted as a critical step.
3. Thanks to recent advances in numerical computing, the last parsec problem appears to be an artefact of oversimplifying assumptions. Galaxies, relic of mergers, are not spherical systems and can retain a high degree of triaxiality or asymmetry. Under these circumstances the hardening of the binary via binary-single stellar encounters appears to have no halt, at least in the cases explored and coalescence timescales are close to 1 to a few Gyr. The issue is not settled yet.
4. It is now possible to track the black hole dynamics during galaxy collisions using state-of-the-art simulations. The dynamics of the interacting galaxies is followed *ab initio*, from the large scale (several kpc) down to the central few parsecs, considering all components - the dark halo, the stellar and gaseous disc, and bulge. This enables us to trace the rise of asymmetries and instabilities in both the stellar and gas components which play a pivotal role in determining whether there is stalling or rapid sinking of the binary.
5. Major gas-rich (wet) mergers are conducive to the formation of close Keplerian binaries. The gas, thanks to its high degree of dissipation, controls the black hole inspiral inside the massive circum-nuclear disc that forms in the end-galaxy. When described as a single phase medium, the gas promotes rapid inspiral before the

disc fragments into stars, and before stellar dynamical friction becomes effective. When the gas is multi-phase and clumpy on various mass scales, the black hole orbit shows a stochastic behaviour. The black holes in this case form a binary on timescales typically between 1 Myr and 100 Myr.

6. Coalescences of middleweight black holes of $\sim 10^4 M_\odot$ at high redshifts $z \sim 10 - 15$ require either very dense, low velocity dispersion stellar environments, or large not yet quantified amounts of gas in unstable forming galaxies.
7. Minor mergers can release the less massive black hole on peripheral orbits in the main galaxy, due to the disruptive action of tidal torques on the less massive galaxy, rising a new problem: the last kpc problem. Gas plays a key role in the process of pairing in minor merger, as it makes the satellite galaxy more resilient against tidal stripping because central gas inflows, triggered during the interaction, steepen the stellar cusp. Due to the fragility of the satellite galaxy, the fate of black holes in minor mergers is uncertain: encounter geometry, gas fraction, degree of gas dissipation are key elements for establishing whether the black hole is a *sinking* or a *wandering* black hole inside the primary galaxy. The prediction is that there is a large scatter in the outcomes.
8. At sub-parsec scales, the Keplerian binary is likely surrounded by a circum-binary disc. When present, gas-assisted inspiral takes place which can be faster than star-driven inspiral. Both processes likely co-exist but have never been treated jointly. The black holes are expected to migrate on a timescale controlled by the interplay between the binary tidal torque which tends to clear a cavity (repelling the disc's gas in the immediate vicinity of the binary) and viscous torques in the disc which tend to fill and even overfill the cavity. Gas leaks through the gap and the black holes are surrounded by mini accretion discs. All these processes modify the orbital elements in a complex way. Theoretical models indicate that if there is a sufficiently long-lived inflow of gas at the inner edge of the circum-binary disc, the binary hardens on timescales $\lesssim 10^9$ Gyr or even much less (depending on the previous history).
9. The path to coalescence still remains a complex problem to solve and there is no clear-cut answer. To be conservative, coalescence times range between several Myrs to about several Gyrs.

The field needs to evolve farther along different lines and directions. Here are a few hints:

1. There is need to continue to study not only the growth of black holes along cosmic history, but their dynamics as they are inter-connected. Attempts to follow the dynamics of black holes during the cosmic assembly of galactic halos have been carried on, albeit at much lower resolution than required to track their accretion history and fate (Bellovary et al. 2010). Any effort along this line is central in order to understand the coevolution of black holes with galaxies.
2. Intriguingly enough, the fate of black hole binaries in galaxies takes us back to the unsolved problem of the feeding of black holes in galactic nuclei over cosmic ages, i.e. of the angular momentum barrier present on parsec scales. Dynamical decay, star formation, accretion and their back-reactions are coupled. Star formation makes the ISM multi-phase and turbulent. Supernova and AGN feed-back may heat/remove gas and the consequences of these effects on black hole migration have not been quantified yet, during orbital evolution.
3. Dual, binary and recoiling AGN and also triple AGN are important observational targets. There is the need to improve upon observational strategies for identifying

binary and recoiling AGN in large surveys, assisted by tailored and coordinated hydro-dynamical simulations.

4. Black hole migration in circum-binary disc is a challenging problem which deserves constant attention. Binary eccentricity growth, accretion and outflows, are processes that affect the dynamics and stability of the system as a whole. Understanding the nature of torques in multi-phase models of circum-nuclear discs will become central in order to extrapolate the black hole migration timescale from the parsec scale down to the domain controlled by gravitational wave inspiral, and to assess the observability of sub-parsec binaries during the phases which anticipate the merging.

Acknowledgements I would like to thank my collaborators Simone Callegari, Massimo Dotti, Davide Fiacconi, Alessandro Lupi, Lucio Mayer, Constanze Roedig, Alberto Sesana and Marta Volonteri for many useful and illuminating discussions over the years. I would like also to thank the International Space Science Institute for kind hospitality.

References

- P. Amaro-Seoane, S. Aoudia, S. Babak, P. Binétruy, E. Berti, A. Bohé, C. Caprini, M. Colpi, N. J. Cornish, K. Danzmann, J.-F. Dufaux, J. Gair, I. Hinder, O. Jennrich, P. Jetzer, A. Klein, R. N. Lang, A. Lobo, T. Littenberg, S. T. McWilliams, G. Nelemans, A. Petiteau, E. K. Porter, B. F. Schutz, A. Sesana, R. Stebbins, T. Sumner, M. Vallisneri, S. Vitale, M. Volonteri, H. Ward, and B. Wardell. eLISA: Astrophysics and cosmology in the millihertz regime. *GW Notes, Vol. 6, p. 4-110*, 6:4–110, May 2013.
- P. J. Armitage. *Astrophysics of Planet Formation*. October 2013.
- P. J. Armitage and P. Natarajan. Accretion during the Merger of Supermassive Black Holes. *Astrophys. J.*, 567:L9–L12, March 2002. doi: 10.1086/339770.
- P. J. Armitage and P. Natarajan. Eccentricity of Supermassive Black Hole Binaries Coalescing from Gas-rich Mergers. *Astrophys. J.*, 634:921–927, December 2005. doi: 10.1086/497108.
- P. Artymowicz and S. H. Lubow. Dynamics of binary-disk interaction. I: Resonances and disk gap sizes. *Astrophys. J.*, 421:651–667, February 1994. doi: 10.1086/173679.
- P. Artymowicz and S. H. Lubow. Mass Flow through Gaps in Circumbinary Disks. *Astrophys. J.*, 467:L77, August 1996. doi: 10.1086/310200.
- M. C. Begelman, R. D. Blandford, and M. J. Rees. Massive black hole binaries in active galactic nuclei. *Nature*, 287:307–309, September 1980. doi: 10.1038/287307a0.
- J. M. Bellovary, F. Governato, T. R. Quinn, J. Wadsley, S. Shen, and M. Volonteri. Wandering Black Holes in Bright Disk Galaxy Halos. *Astrophys. J.*, 721:L148–L152, October 2010. doi: 10.1088/2041-8205/721/2/L148.
- P. Berczik, D. Merritt, R. Spurzem, and H.-P. Bischof. Efficient Merger of Binary Supermassive Black Holes in Nonaxisymmetric Galaxies. *Astrophys. J.*, 642:L21–L24, May 2006. doi: 10.1086/504426.
- O. Blaes, M. H. Lee, and A. Socrates. The Kozai Mechanism and the Evolution of Binary Supermassive Black Holes. *Astrophys. J.*, 578:775–786, October 2002. doi: 10.1086/342655.
- T. Bode, R. Haas, T. Bogdanović, P. Laguna, and D. Shoemaker. Relativistic Mergers of Supermassive Black Holes and Their Electromagnetic Signatures. *Astrophys. J.*, 715: 1117–1131, June 2010. doi: 10.1088/0004-637X/715/2/1117.
- T. Bogdanović, C. S. Reynolds, and M. C. Miller. Alignment of the Spins of Supermassive Black Holes Prior to Coalescence. *Astrophys. J.*, 661:L147–L150, June 2007. doi: 10.1086/518769.
- M. Boylan-Kolchin, C.-P. Ma, and E. Quataert. Dynamical friction and galaxy merging timescales. *MNRAS*, 383:93–101, January 2008. doi: 10.1111/j.1365-2966.2007.12530.x.
- S. Callegari, L. Mayer, S. Kazantzidis, M. Colpi, F. Governato, T. Quinn, and J. Wadsley. Pairing of Supermassive Black Holes in Unequal-Mass Galaxy Mergers. *Astrophys. J.*, 696:L89–L92, May 2009. doi: 10.1088/0004-637X/696/1/L89.

-
- S. Callegari, S. Kazantzidis, L. Mayer, M. Colpi, J. M. Bellovary, T. Quinn, and J. Wadsley. Growing Massive Black Hole Pairs in Minor Mergers of Disk Galaxies. *Astrophys. J.*, 729: 85, March 2011. doi: 10.1088/0004-637X/729/2/85.
- J. Centrella, J. G. Baker, B. J. Kelly, and J. R. van Meter. Black-hole binaries, gravitational waves, and numerical relativity. *Reviews of Modern Physics*, 82:3069–3119, October 2010. doi: 10.1103/RevModPhys.82.3069.
- S. Chandrasekhar. Dynamical Friction. I. General Considerations: the Coefficient of Dynamical Friction. *Astrophys. J.*, 97:255, March 1943. doi: 10.1086/144517.
- D. Chapon, L. Mayer, and R. Teyssier. Hydrodynamics of galaxy mergers with supermassive black holes: is there a last parsec problem? *MNRAS*, 429:3114–3122, March 2013. doi: 10.1093/mnras/sts568.
- M. Colpi and M. Dotti. Massive Binary Black Holes in the Cosmic Landscape. *Advanced Science Letters*, 4:181–203, February 2011. doi: 10.1166/asl.2011.1205.
- M. Colpi, L. Mayer, and F. Governato. Dynamical Friction and the Evolution of Satellites in Virialized Halos: The Theory of Linear Response. *Astrophys. J.*, 525:720–733, November 1999. doi: 10.1086/307952.
- M. Colpi, S. Callegari, M. Dotti, and L. Mayer. Massive black hole binary evolution in gas-rich mergers. *Classical and Quantum Gravity*, 26(9):094029, May 2009. doi: 10.1088/0264-9381/26/9/094029.
- J. M. Comerford and J. E. Greene. Offset Active Galactic Nuclei as Tracers of Galaxy Mergers and Supermassive Black Hole Growth. *Astrophys. J.*, 789:112, July 2014. doi: 10.1088/0004-637X/789/2/112.
- J. Cuadra, P. J. Armitage, R. D. Alexander, and M. C. Begelman. Massive black hole binary mergers within subparsec scale gas discs. *MNRAS*, 393:1423–1432, March 2009. doi: 10.1111/j.1365-2966.2008.14147.x.
- R. Decarli, M. Dotti, M. Fumagalli, P. Tsalmanza, C. Montuori, E. Lusso, D. W. Hogg, and J. X. Prochaska. The nature of massive black hole binary candidates - I. Spectral properties and evolution. *MNRAS*, 433:1492–1504, August 2013. doi: 10.1093/mnras/stt831.
- L. del Valle and A. Escala. Binary-Disk Interaction: Gap-opening Criteria. *Astrophys. J.*, 761: 31, December 2012. doi: 10.1088/0004-637X/761/1/31.
- L. del Valle and A. Escala. Binary-Disk Interaction. II. Gap-opening Criteria for Unequal-mass Binaries. *Astrophys. J.*, 780:84, January 2014. doi: 10.1088/0004-637X/780/1/84.
- B. Devecchi, E. Rasia, M. Dotti, M. Volonteri, and M. Colpi. Imprints of recoiling massive black holes on the hot gas of early-type galaxies. *MNRAS*, 394:633–640, April 2009. doi: 10.1111/j.1365-2966.2008.14329.x.
- T. Di Matteo, V. Springel, and L. Hernquist. Energy input from quasars regulates the growth and activity of black holes and their host galaxies. *Nature*, 433:604–607, February 2005. doi: 10.1038/nature03335.
- D. J. D’Orazio, Z. Haiman, and A. MacFadyen. Accretion into the central cavity of a circumbinary disc. *MNRAS*, 436:2997–3020, December 2013. doi: 10.1093/mnras/stt1787.
- M. Dotti, M. Colpi, and F. Haardt. Laser Interferometer Space Antenna double black holes: dynamics in gaseous nuclear discs. *MNRAS*, 367:103–112, March 2006. doi: 10.1111/j.1365-2966.2005.09956.x.
- M. Dotti, M. Colpi, F. Haardt, and L. Mayer. Supermassive black hole binaries in gaseous and stellar circumnuclear discs: orbital dynamics and gas accretion. *MNRAS*, 379:956–962, August 2007. doi: 10.1111/j.1365-2966.2007.12010.x.
- M. Dotti, M. Ruzkowski, L. Paredi, M. Colpi, M. Volonteri, and F. Haardt. Dual black holes in merger remnants - I. Linking accretion to dynamics. *MNRAS*, 396:1640–1646, July 2009. doi: 10.1111/j.1365-2966.2009.14840.x.
- M. Dotti, M. Volonteri, A. Perego, M. Colpi, M. Ruzkowski, and F. Haardt. Dual black holes in merger remnants - II. Spin evolution and gravitational recoil. *MNRAS*, 402:682–690, February 2010. doi: 10.1111/j.1365-2966.2009.15922.x.
- M. Dotti, A. Sesana, and R. Decarli. Massive Black Hole Binaries: Dynamical Evolution and Observational Signatures. *Advances in Astronomy*, 2012:940568, 2012. doi: 10.1155/2012/940568.
- P. C. Duffell, Z. Haiman, A. I. MacFadyen, D. J. D’Orazio, and B. D. Farris. Type II Migration is not Locked to Viscous Disk Evolution. *ArXiv e-prints*, May 2014.
- eLISA Consortium. The Gravitational Universe, the science theme selected by ESA as L3 mission. *ArXiv e-prints*, May 2013.

- M. Eracleous, T. A. Boroson, J. P. Halpern, and J. Liu. A Large Systematic Search for Recoiling and Close Supermassive Binary Black Holes. *ArXiv e-prints*, June 2011.
- A. Escala, R. B. Larson, P. S. Coppi, and D. Mardones. The Role of Gas in the Merging of Massive Black Holes in Galactic Nuclei. II. Black Hole Merging in a Nuclear Gas Disk. *Astrophys. J.*, 630:152–166, September 2005. doi: 10.1086/431747.
- B. D. Farris, P. Duffell, A. I. MacFadyen, and Z. Haiman. Binary Black Hole Accretion from a Circumbinary Disk: Gas Dynamics inside the Central Cavity. *Astrophys. J.*, 783:134, March 2014. doi: 10.1088/0004-637X/783/2/134.
- L. Ferrarese and H. Ford. Supermassive Black Holes in Galactic Nuclei: Past, Present and Future Research. *Space Science Reviews*, 116:523–624, February 2005. doi: 10.1007/s11214-005-3947-6.
- L. Ferrarese, P. Côté, E. Dalla Bontà, E. W. Peng, D. Merritt, A. Jordán, J. P. Blakeslee, M. Hasegan, S. Mei, S. Piatek, J. L. Tonry, and M. J. West. A Fundamental Relation between Compact Stellar Nuclei, Supermassive Black Holes, and Their Host Galaxies. *Astrophys. J.*, 644:L21–L24, June 2006. doi: 10.1086/505388.
- D. Fiacconi, L. Mayer, R. Roškar, and M. Colpi. Massive Black Hole Pairs in Clumpy, Self-gravitating Circumnuclear Disks: Stochastic Orbital Decay. *Astrophys. J.*, 777:L14, November 2013. doi: 10.1088/2041-8205/777/1/L14.
- D. Gerosa and A. Sesana. Missing black holes in brightest cluster galaxies as evidence for the occurrence of superkicks in nature. *ArXiv e-prints*, May 2014.
- A. M. Ghez, S. Salim, N. N. Weinberg, J. R. Lu, T. Do, J. K. Dunn, K. Matthews, M. R. Morris, S. Yelda, E. E. Becklin, T. Kremenek, M. Milosavljevic, and J. Naiman. Measuring Distance and Properties of the Milky Way’s Central Supermassive Black Hole with Stellar Orbits. *Astrophys. J.*, 689:1044–1062, December 2008. doi: 10.1086/592738.
- S. Gillessen, F. Eisenhauer, S. Trippe, T. Alexander, R. Genzel, F. Martins, and T. Ott. Monitoring Stellar Orbits Around the Massive Black Hole in the Galactic Center. *Astrophys. J.*, 692:1075–1109, February 2009. doi: 10.1088/0004-637X/692/2/1075.
- A. Gould and H.-W. Rix. Binary Black Hole Mergers from Planet-like Migrations. *Astrophys. J.*, 532:L29–L32, March 2000. doi: 10.1086/312562.
- F. Governato, M. Colpi, and L. Maraschi. The fate of central black holes in merging galaxies. *MNRAS*, 271:317, November 1994.
- A. Gualandris and D. Merritt. Ejection of Supermassive Black Holes from Galaxy Cores. *Astrophys. J.*, 678:780–797, May 2008. doi: 10.1086/586877.
- K. Gültekin, D. O. Richstone, K. Gebhardt, T. R. Lauer, S. Tremaine, M. C. Aller, R. Bender, A. Dressler, S. M. Faber, A. V. Filippenko, R. Green, L. C. Ho, J. Kormendy, J. Magorrian, J. Pinkney, and C. Siopis. The M - σ and M - L Relations in Galactic Bulges, and Determinations of Their Intrinsic Scatter. *Astrophys. J.*, 698:198–221, June 2009. doi: 10.1088/0004-637X/698/1/198.
- Z. Haiman, B. Kocsis, and K. Menou. The Population of Viscosity- and Gravitational Wave-driven Supermassive Black Hole Binaries Among Luminous Active Galactic Nuclei. *Astrophys. J.*, 700:1952–1969, August 2009. doi: 10.1088/0004-637X/700/2/1952.
- N. Häring and H.-W. Rix. On the Black Hole Mass-Bulge Mass Relation. *Astrophys. J.*, 604:L89–L92, April 2004. doi: 10.1086/383567.
- K. Hayasaki. A New Mechanism for Massive Binary Black-Hole Evolution. *PASJ*, 61:65–, February 2009.
- K. Hayasaki, S. Mineshige, and H. Sudou. Binary Black Hole Accretion Flows in Merged Galactic Nuclei. *PASJ*, 59:427–441, April 2007.
- K. Hayasaki, S. Mineshige, and L. C. Ho. A Supermassive Binary Black Hole with Triple Disks. *Astrophys. J.*, 682:1134–1140, August 2008. doi: 10.1086/588837.
- K. Hayasaki, H. Saito, and S. Mineshige. Binary Black Hole Accretion Flows From a Misaligned Circumbinary Disk. *PASJ*, 65:86, August 2013.
- A. Heger, C. L. Fryer, S. E. Woosley, N. Langer, and D. H. Hartmann. How Massive Single Stars End Their Life. *Astrophys. J.*, 591:288–300, July 2003. doi: 10.1086/375341.
- L. Hoffman and A. Loeb. Dynamics of triple black hole systems in hierarchically merging massive galaxies. *MNRAS*, 377:957–976, May 2007. doi: 10.1111/j.1365-2966.2007.11694.x.
- P. F. Hopkins, L. Hernquist, T. J. Cox, T. Di Matteo, B. Robertson, and V. Springel. A Unified, Merger-driven Model of the Origin of Starbursts, Quasars, the Cosmic X-Ray Background, Supermassive Black Holes, and Galaxy Spheroids. *ApJS*, 163:1–49, March 2006. doi: 10.1086/499298.

- P. F. Hopkins, T. J. Cox, L. Hernquist, D. Narayanan, C. C. Hayward, and N. Murray. Star formation in galaxy mergers with realistic models of stellar feedback and the interstellar medium. *MNRAS*, 430:1901–1927, April 2013. doi: 10.1093/mnras/stt017.
- P. B. Ivanov, J. C. B. Papaloizou, and A. G. Polnarev. The evolution of a supermassive binary caused by an accretion disc. *MNRAS*, 307:79–90, July 1999. doi: 10.1046/j.1365-8711.1999.02623.x.
- S. Kazantzidis, L. Mayer, M. Colpi, P. Madau, V. P. Debattista, J. Wadsley, J. Stadel, T. Quinn, and B. Moore. The Fate of Supermassive Black Holes and the Evolution of the M_{BH} - σ Relation in Merging Galaxies: The Effect of Gaseous Dissipation. *Astrophys. J.*, 623:L67–L70, April 2005. doi: 10.1086/430139.
- F. M. Khan, A. Just, and D. Merritt. Efficient Merger of Binary Supermassive Black Holes in Merging Galaxies. *Astrophys. J.*, 732:89, May 2011. doi: 10.1088/0004-637X/732/2/89.
- F. M. Khan, I. Berentzen, P. Berczik, A. Just, L. Mayer, K. Nitadori, and S. Callegari. Formation and Hardening of Supermassive Black Hole Binaries in Minor Mergers of Disk Galaxies. *Astrophys. J.*, 756:30, September 2012a. doi: 10.1088/0004-637X/756/1/30.
- F. M. Khan, M. Preto, P. Berczik, I. Berentzen, A. Just, and R. Spurzem. Mergers of Unequal-mass Galaxies: Supermassive Black Hole Binary Evolution and Structure of Merger Remnants. *Astrophys. J.*, 749:147, April 2012b. doi: 10.1088/0004-637X/749/2/147.
- F. M. Khan, K. Holley-Bockelmann, P. Berczik, and A. Just. Supermassive Black Hole Binary Evolution in Axisymmetric Galaxies: The Final Parsec Problem is Not a Problem. *Astrophys. J.*, 773:100, August 2013. doi: 10.1088/0004-637X/773/2/100.
- H. Kim, W.-T. Kim, and F. J. Sánchez-Salcedo. Dynamical Friction of Double Perturbers in a Gaseous Medium. *Astrophys. J.*, 679:L33–L36, May 2008. doi: 10.1086/589149.
- B. Kocsis, Z. Haiman, and A. Loeb. Gas pile-up, gap overflow and Type 1.5 migration in circumbinary discs: application to supermassive black hole binaries. *MNRAS*, 427:2680–2700, December 2012. doi: 10.1111/j.1365-2966.2012.22118.x.
- S. Komossa. Observational evidence for binary black holes and active double nuclei. *Memorie SIAI*, 77:733, 2006.
- S. Komossa. Recoiling Black Holes: Electromagnetic Signatures, Candidates, and Astrophysical Implications. *Advances in Astronomy*, 2012:364973, 2012. doi: 10.1155/2012/364973.
- J. Kormendy and L. C. Ho. Coevolution (Or Not) of Supermassive Black Holes and Host Galaxies. *ARA&A*, 51:511–553, August 2013. doi: 10.1146/annurev-astro-082708-101811.
- M. Koss, R. Mushotzky, E. Treister, S. Veilleux, R. Vasudevan, and M. Trippe. Understanding Dual Active Galactic Nucleus Activation in the nearby Universe. *Astrophys. J.*, 746:L22, February 2012. doi: 10.1088/2041-8205/746/2/L22.
- G. Kulkarni and A. Loeb. Formation of galactic nuclei with multiple supermassive black holes at high redshifts. *MNRAS*, 422:1306–1323, May 2012. doi: 10.1111/j.1365-2966.2012.20699.x.
- F. K. Liu, S. Li, and S. Komossa. A Milliparsec Supermassive Black Hole Binary Candidate in the Galaxy SDSS J120136.02+300305.5. *Astrophys. J.*, 786:103, May 2014. doi: 10.1088/0004-637X/786/2/103.
- X. Liu, Y. Shen, M. A. Strauss, and L. Hao. Active Galactic Nucleus Pairs from the Sloan Digital Sky Survey. I. The Frequency on ~ 5 –100 kpc Scales. *Astrophys. J.*, 737:101, August 2011. doi: 10.1088/0004-637X/737/2/101.
- X. Liu, F. Civano, Y. Shen, P. Green, J. E. Greene, and M. A. Strauss. Chandra X-Ray and Hubble Space Telescope Imaging of Optically Selected Kiloparsec-scale Binary Active Galactic Nuclei. I. Nature of the Nuclear Ionizing Sources. *Astrophys. J.*, 762:110, January 2013. doi: 10.1088/0004-637X/762/2/110.
- G. Lodato, S. Nayakshin, A. R. King, and J. E. Pringle. Black hole mergers: can gas discs solve the ‘final parsec’ problem? *MNRAS*, 398:1392–1402, September 2009. doi: 10.1111/j.1365-2966.2009.15179.x.
- C. O. Lousto and Y. Zlochower. Black hole binary remnant mass and spin: A new phenomenological formula. *ArXiv e-prints*, December 2013.
- E. Lusso, R. Decarli, M. Dotti, C. Montuori, D. W. Hogg, P. Tsalmanza, M. Fumagalli, and J. X. Prochaska. The nature of massive black hole binary candidates - II. Spectral energy distribution atlas. *MNRAS*, 441:316–332, June 2014. doi: 10.1093/mnras/stu572.
- A. I. MacFadyen and M. Milosavljević. An Eccentric Circumbinary Accretion Disk and the Detection of Binary Massive Black Holes. *Astrophys. J.*, 672:83–93, January 2008. doi: 10.1086/523869.

- A. Marconi and L. K. Hunt. The Relation between Black Hole Mass, Bulge Mass, and Near-Infrared Luminosity. *Astrophys. J.*, 589:L21–L24, May 2003. doi: 10.1086/375804.
- A. Marconi, G. Risaliti, R. Gilli, L. K. Hunt, R. Maiolino, and M. Salvati. Local supermassive black holes, relics of active galactic nuclei and the X-ray background. *MNRAS*, 351:169–185, June 2004. doi: 10.1111/j.1365-2966.2004.07765.x.
- L. Mayer. Massive black hole binaries in gas-rich galaxy mergers; multiple regimes of orbital decay and interplay with gas inflows. *Classical and Quantum Gravity*, 30(24):244008, December 2013. doi: 10.1088/0264-9381/30/24/244008.
- L. Mayer, S. Kazantzidis, P. Madau, M. Colpi, T. Quinn, and J. Wadsley. Rapid Formation of Supermassive Black Hole Binaries in Galaxy Mergers with Gas. *Science*, 316:1874–, June 2007. doi: 10.1126/science.1141858.
- A. Merloni and S. Heinz. *Evolution of Active Galactic Nuclei*, page 503. March 2013. doi: 10.1007/978-94-007-5609-011.
- D. Merritt. *Dynamics and Evolution of Galactic Nuclei*. July 2013a.
- D. Merritt. Loss-cone dynamics. *Classical and Quantum Gravity*, 30(24):244005, December 2013b. doi: 10.1088/0264-9381/30/24/244005.
- D. Merritt and M. Milosavljević. Massive Black Hole Binary Evolution. *Living Reviews in Relativity*, 8:8, November 2005. doi: 10.12942/lrr-2005-8.
- D. Merritt and M. Y. Poon. Chaotic Loss Cones and Black Hole Fueling. *Astrophys. J.*, 606:788–798, May 2004. doi: 10.1086/382497.
- D. Merritt, J. D. Schnittman, and S. Komossa. Hypercompact Stellar Systems Around Recoiling Supermassive Black Holes. *Astrophys. J.*, 699:1690–1710, July 2009. doi: 10.1088/0004-637X/699/2/1690.
- J. C. Mihos and L. Hernquist. Gasdynamics and Starbursts in Major Mergers. *Astrophys. J.*, 464:641, June 1996. doi: 10.1086/177353.
- M. Milosavljević and D. Merritt. Formation of Galactic Nuclei. *Astrophys. J.*, 563:34–62, December 2001. doi: 10.1086/323830.
- M. Milosavljević and D. Merritt. Long-Term Evolution of Massive Black Hole Binaries. *Astrophys. J.*, 596:860–878, October 2003. doi: 10.1086/378086.
- C. Montuori, M. Dotti, F. Haardt, M. Colpi, and R. Decarli. Search for sub-parsec massive binary black holes through line diagnosis - II. *MNRAS*, 425:1633–1639, September 2012. doi: 10.1111/j.1365-2966.2012.21530.x.
- J. F. Navarro, C. S. Frenk, and S. D. M. White. The Structure of Cold Dark Matter Halos. *Astrophys. J.*, 462:563, May 1996. doi: 10.1086/177173.
- S. C. Noble, B. C. Mundim, H. Nakano, J. H. Krolik, M. Campanelli, Y. Zlochower, and N. Yunes. Circumbinary Magnetohydrodynamic Accretion into Inspiral Binary Black Holes. *Astrophys. J.*, 755:51, August 2012. doi: 10.1088/0004-637X/755/1/51.
- K. Omukai and F. Palla. On the Formation of Massive Primordial Stars. *Astrophys. J.*, 561:L55–L58, November 2001. doi: 10.1086/324410.
- E. C. Ostriker. Dynamical Friction in a Gaseous Medium. *Astrophys. J.*, 513:252–258, March 1999. doi: 10.1086/306858.
- F. Özel, D. Psaltis, R. Narayan, and J. E. McClintock. The Black Hole Mass Distribution in the Galaxy. *Astrophys. J.*, 725:1918–1927, December 2010. doi: 10.1088/0004-637X/725/2/1918.
- H. B. Perets, C. Hopman, and T. Alexander. Massive Perturber-driven Interactions between Stars and a Massive Black Hole. *Astrophys. J.*, 656:709–720, February 2007. doi: 10.1086/510377.
- M. Preto, I. Berentzen, P. Berczik, and R. Spurzem. Fast Coalescence of Massive Black Hole Binaries from Mergers of Galactic Nuclei: Implications for Low-frequency Gravitational-wave Astrophysics. *Astrophys. J.*, 732:L26, May 2011. doi: 10.1088/2041-8205/732/2/L26.
- J. E. Pringle. The properties of external accretion discs. *MNRAS*, 248:754–759, February 1991.
- G. D. Quinlan. The time-scale for core collapse in spherical star clusters. *New Astronomy*, 1:255–270, November 1996. doi: 10.1016/S1384-1076(96)00018-8.
- R. R. Rafikov. Structure and Evolution of Circumbinary Disks around Supermassive Black Hole Binaries. *Astrophys. J.*, 774:144, September 2013. doi: 10.1088/0004-637X/774/2/144.
- A. E. Reines, J. E. Greene, and M. Geha. Dwarf Galaxies with Optical Signatures of Active Massive Black Holes. *Astrophys. J.*, 775:116, October 2013. doi: 10.1088/0004-637X/775/2/116.

- L. Rezzolla, E. Barausse, E. N. Dorband, D. Pollney, C. Reisswig, J. Seiler, and S. Husa. Final spin from the coalescence of two black holes. *Phys. Rev. D*, 78(4):044002, August 2008. doi: 10.1103/PhysRevD.78.044002.
- C. Roedig, M. Dotti, A. Sesana, J. Cuadra, and M. Colpi. Limiting eccentricity of subparsec massive black hole binaries surrounded by self-gravitating gas discs. *MNRAS*, 415:3033–3041, August 2011. doi: 10.1111/j.1365-2966.2011.18927.x.
- C. Roedig, A. Sesana, M. Dotti, J. Cuadra, P. Amaro-Seoane, and F. Haardt. Evolution of binary black holes in self gravitating discs. Dissecting the torques. *Astron. Astrophys.*, 545:A127, September 2012. doi: 10.1051/0004-6361/201219986.
- R. Roškar, L. Mayer, D. Fiacconi, S. Kazantzidis, T. R. Quinn, and J. Wadsley. Orbital Decay of Supermassive Black Hole Binaries in Clumpy Multiphase Merger Remnants. *ArXiv e-prints*, June 2014.
- B. S. Sathyaprakash and B. F. Schutz. Physics, Astrophysics and Cosmology with Gravitational Waves. *Living Reviews in Relativity*, 12:2, March 2009. doi: 10.12942/lrr-2009-2.
- D. R. G. Schleicher, F. Palla, A. Ferrara, D. Galli, and M. Latif. Massive black hole factories: Supermassive and quasi-star formation in primordial halos. *Astron. Astrophys.*, 558:A59, October 2013. doi: 10.1051/0004-6361/201321949.
- J. D. Schnittman. Electromagnetic counterparts to black hole mergers. *Classical and Quantum Gravity*, 28(9):094021, May 2011. doi: 10.1088/0264-9381/28/9/094021.
- N. Scott and A. W. Graham. Updated Mass Scaling Relations for Nuclear Star Clusters and a Comparison to Supermassive Black Holes. *Astrophys. J.*, 763:76, February 2013. doi: 10.1088/0004-637X/763/2/76.
- A. Sesana. Self Consistent Model for the Evolution of Eccentric Massive Black Hole Binaries in Stellar Environments: Implications for Gravitational Wave Observations. *Astrophys. J.*, 719:851–864, August 2010. doi: 10.1088/0004-637X/719/1/851.
- A. Seth, M. Agüeros, D. Lee, and A. Basu-Zych. The Coincidence of Nuclear Star Clusters and Active Galactic Nuclei. *Astrophys. J.*, 678:116–130, May 2008. doi: 10.1086/528955.
- N. I. Shakura and R. A. Sunyaev. Black holes in binary systems. Observational appearance. *Astron. Astrophys.*, 24:337–355, 1973.
- J.-M. Shi, J. H. Krolik, S. H. Lubow, and J. F. Hawley. Three-dimensional Magnetohydrodynamic Simulations of Circumbinary Accretion Disks: Disk Structures and Angular Momentum Transport. *Astrophys. J.*, 749:118, April 2012. doi: 10.1088/0004-637X/749/2/118.
- D. Syer and C. J. Clarke. Satellites in discs: regulating the accretion luminosity. *MNRAS*, 277:758–766, December 1995.
- G. Taffoni, L. Mayer, M. Colpi, and F. Governato. On the life and death of satellite haloes. *MNRAS*, 341:434–448, May 2003. doi: 10.1046/j.1365-8711.2003.06395.x.
- H. Tanaka, T. Takeuchi, and W. R. Ward. Three-Dimensional Interaction between a Planet and an Isothermal Gaseous Disk. I. Corotation and Lindblad Torques and Planet Migration. *Astrophys. J.*, 565:1257–1274, February 2002. doi: 10.1086/324713.
- S. Van Wassenhove, M. Volonteri, L. Mayer, M. Dotti, J. Bellovary, and S. Callegari. Observability of Dual Active Galactic Nuclei in Merging Galaxies. *Astrophys. J.*, 748:L7, March 2012. doi: 10.1088/2041-8205/748/1/L7.
- S. Van Wassenhove, P. R. Capelo, M. Volonteri, M. Dotti, J. M. Bellovary, L. Mayer, and F. Governato. Nuclear coups: dynamics of black holes in galaxy mergers. *MNRAS*, February 2014. doi: 10.1093/mnras/stu024.
- E. Vasiliev, F. Antonini, and D. Merritt. The final-parsec problem in non-spherical galaxies revisited. *ArXiv e-prints*, November 2013.
- M. Vestergaard, X. Fan, C. A. Tremonti, P. S. Osmer, and G. T. Richards. Mass Functions of the Active Black Holes in Distant Quasars from the Sloan Digital Sky Survey Data Release 3. *Astrophys. J.*, 674:L1–L4, February 2008. doi: 10.1086/528981.
- M. Volonteri. Formation of supermassive black holes. *A&A Rev.*, 18:279–315, July 2010. doi: 10.1007/s00159-010-0029-x.
- M. Volonteri and P. Natarajan. Journey to the $M_{BH}-\sigma$ relation: the fate of low-mass black holes in the Universe. *MNRAS*, 400:1911–1918, December 2009. doi: 10.1111/j.1365-2966.2009.15577.x.
- M. Volonteri, F. Haardt, and P. Madau. The Assembly and Merging History of Supermassive Black Holes in Hierarchical Models of Galaxy Formation. *Astrophys. J.*, 582:559–573, January 2003. doi: 10.1086/344675.
- L. Wang, P. Berczik, R. Spurzem, and M. B. N. Kouwenhoven. The Link between Ejected Stars, Hardening and Eccentricity Growth of Super Massive Black Holes in Galactic Nuclei.

- Astrophys. J.*, 780:164, January 2014. doi: 10.1088/0004-637X/780/2/164.
- S. D. M. White and M. J. Rees. Core condensation in heavy halos - A two-stage theory for galaxy formation and clustering. *MNRAS*, 183:341–358, May 1978.
- Q. Yu. Evolution of massive binary black holes. *MNRAS*, 331:935–958, April 2002. doi: 10.1046/j.1365-8711.2002.05242.x.